

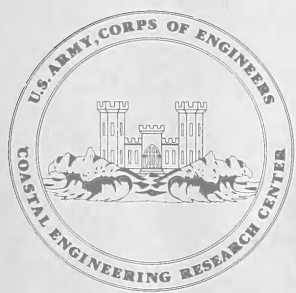
U.S. Army  
Coast. Eng. Res. Ctr.  
MR 80-6

WHOI  
DOCUMENT  
COLLECTION

# A Numerical Model for Predicting Shoreline Changes

by  
Bernard Le Mehaute and Mills Soldate

MISCELLANEOUS REPORT NO. 80-6  
JULY 1980



Approved for public release;  
distribution unlimited.

Prepared for  
U.S. ARMY, CORPS OF ENGINEERS  
COASTAL ENGINEERING  
RESEARCH CENTER

Kingman Building  
Fort Belvoir, Va. 22060

TC  
203  
10581  
MR 80-6

Reprint or republication of any of this material shall give appropriate credit to the U.S. Army Coastal Engineering Research Center.

Limited free distribution within the United States of single copies of this publication has been made by this Center. Additional copies are available from:

*National Technical Information Service  
ATTN: Operations Division  
5285 Port Royal Road  
Springfield, Virginia 22161*

The findings in this report are not to be construed as an official Department of the Army position unless so designated by other authorized documents.



REPORT DOCUMENTATION PAGE		READ INSTRUCTIONS BEFORE COMPLETING FORM
1. REPORT NUMBER MR 80-6	2. GOVT ACCESSION NO.	3. RECIPIENT'S CATALOG NUMBER
4. TITLE (and Subtitle) A NUMERICAL MODEL FOR PREDICTING SHORELINE CHANGES		5. TYPE OF REPORT & PERIOD COVERED Miscellaneous Report
		6. PERFORMING ORG. REPORT NUMBER Tetra Tech Report No. TC-831
7. AUTHOR(s) Bernard Le Mehaute and Mills Soldate		8. CONTRACT OR GRANT NUMBER(s) DACW72-7T-C-0002
9. PERFORMING ORGANIZATION NAME AND ADDRESS Tetra Tech, Inc. 630 North Rosemead Boulevard Pasadena, California 91107		10. PROGRAM ELEMENT, PROJECT, TASK AREA & WORK UNIT NUMBERS F31551
11. CONTROLLING OFFICE NAME AND ADDRESS Department of the Army Coastal Engineering Research Center Kingman Building, Fort Belvoir, Virginia 22060		12. REPORT DATE July 1980
		13. NUMBER OF PAGES 72
14. MONITORING AGENCY NAME & ADDRESS (if different from Controlling Office)		15. SECURITY CLASS. (of this report) UNCLASSIFIED
		15a. DECLASSIFICATION/DOWNGRADING SCHEDULE
16. DISTRIBUTION STATEMENT (of this Report) Approved for public release; distribution unlimited.		
17. DISTRIBUTION STATEMENT (of the abstract entered in Block 20, if different from Report)		
18. SUPPLEMENTARY NOTES		
19. KEY WORDS (Continue on reverse side if necessary and identify by block number)		
Currents Great Lakes Holland Harbor, Michigan	Numerical model Shore structures Shoreline changes	Shoreline evolution Wave diffraction Wave refraction
20. ABSTRACT (Continue on reverse side if necessary and identify by block number) A mathematical model for long-term, three-dimensional shoreline evolution is developed. The combined effects of variations of sea level; wave refraction and diffraction; loss of sand by density currents during storms, by rip currents, and by wind; bluff erosion and berm accretion; effects of manmade structures such as long groin or navigational structures; and beach nourishment are all taken into account. A computer program is developed with various subroutines which permit modification as the state-of-the-art progresses. The program is applied to a test case at Holland Harbor, Michigan.		



## PREFACE

This report is published to provide coastal engineers with a mathematical modeling procedure for predicting shoreline evolution resulting from the construction of navigation and shore structures. The model is calibrated with a test case at Holland Harbor, Michigan. This report is a continuation of an investigation by Le Mehaute and Soldate (1977) to determine the feasibility of applying numerical models to real case situations. The work was carried out under the coastal structures program of the Coastal Engineering Research Center (CERC).

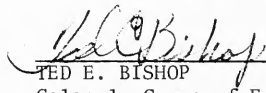
The report was prepared by Bernard Le Mehaute and Mills Soldate, Tetra Tech, Inc., Pasadena, California, under CERC Contract No. DACW72-7T-C-0002.

The authors acknowledge the assistance of Dr. J.R. Weggel, CERC, and C. Johnson, U.S. Army Engineer District, Chicago, for their pertinent comments during this investigation. Informal discussions with Dr. R. Dean, University of Delaware, were very constructive. The contributions of Dr. I. Collins, Dr. C. Sonu, and J. Nelson are also acknowledged, as well as A. Ashley's analysis of the input data.

Dr. J.R. Weggel was the CERC contract monitor for the report, under the general supervision of N.E. Parker, Chief, Engineering Development Division.

Comments on this publication are invited.

Approved for publication in accordance with Public Law 166, 79th Congress, approved 31 July 1945, as supplemented by Public Law 172, 88th Congress, approved 7 November 1963.

  
\_\_\_\_\_  
TED E. BISHOP  
Colonel, Corps of Engineers  
Commander and Director

## CONTENTS

	Page
CONVERSION FACTORS, U.S. CUSTOMARY TO METRIC (SI) . . . . .	6
SYMBOLS AND DEFINITIONS. . . . .	7
I INTRODUCTION . . . . .	9
II THEORETICAL DEVELOPMENTS . . . . .	11
III INPUT DATA . . . . .	31
1. Description and History of Navigation Project at Holland Harbor . . . . .	31
2. Geomorphology . . . . .	33
3. Littoral Materials. . . . .	38
4. Meteorology . . . . .	39
5. Hydrology . . . . .	43
6. Littoral Drift Estimate from Wave Statistics. . . . .	43
7. Analysis of Aerial Photos . . . . .	45
8. Comparisons of Profiles from 1945 and 1975 Surveys. . . . .	46
9. Sediment Budget . . . . .	50
IV CONCLUSIONS AND RECOMMENDATIONS . . . . .	59
LITERATURE CITED . . . . .	62
APPENDIX COMPUTER PROGRAM . . . . .	63

### TABLES

1 History of shoreline positions at Holland, Michigan, from 1950 to 1973, with and without lake level corrections. . . . .	47
2 Summary of cross-sectional changes and computed volumetric changes for 1945 and 1973 surveys. . . . .	50
3 Summary of shoreline accretion rates north of Holland Harbor (1849-1945). . . . .	52
4 Summary of beach area changes south of Holland Harbor . . . . .	56
5 SSMO averages for Holland Harbor. . . . .	59

### FIGURES

1 Coastal zone. . . . .	11
2 Height of bluff or berm . . . . .	12
3 Change of beach profile . . . . .	13
4 Changes of sand volume due to translation of one beach profile. . . . .	14
5 Effects of wave refractions on a curved beach . . . . .	17
6 Diffraction zone notation . . . . .	20
7 Notation for diffraction study. . . . .	21

CONTENTS

FIGURES--Continued

	Page
8 Initial shoreline and incoming wave direction (A); shorelines at successive times of $1\Delta t$ , $2\Delta t$ , $5\Delta t$ , $10\Delta t$ , and $20\Delta t$ (B) . . . . .	24
9 Shorelines at successive times of $5\Delta t$ , $10\Delta t$ , and $15\Delta t$ (A); shorelines for time $2\Delta t$ (B). . . . .	25
10 Initial shoreline and incoming wave direction (A); computed and minimal shorelines for finite-difference scheme of time $1\Delta t$ (B) . . .	27
11 Transport function $Q(\alpha_0) = \cos \alpha_0 \sin z\alpha_0$ for selected values of $z$ . . .	28
12 Layout of shoreline reaches characterized by different beach conditions. . . . .	32
13 Nearshore bathymetry, Holland Harbor . . . . .	34
14 Beach profile summaries for Holland Harbor . . . . .	35
15 Holland Harbor nearshore bathymetry. . . . .	37
16 Conditions at Holland Harbor entrance before dredging in 1973 and 1974. . . . .	40
17 Wind rose for an average 12-month period and for an average 9-month ice-free period for southern Lake Michigan. . . . .	41
18 Wave rose for an average 12-month period and for an assumed 9-month ice-free period for southern Lake Michigan. . . . .	41
19 Wave height exceedance probabilities (9-month ice-free period) . . . .	42
20 Variations of probability of various wave heights with months of the year. . . . .	42
21 Mean monthly lake levels since 1920. . . . .	44
22 Monthly variations of computed gross and net littoral drifts for Holland, Michigan . . . . .	45
23 Shoreline positions at Holland, Michigan, in 1973, as determined by aerial photos. . . . .	48
24 Smoothed average rates of shoreline erosion and accretion at Holland, Michigan . . . . .	49
25 Historical shorelines north of Holland, Michigan, from 1849 to 1945. . .	51
26 Summary of sand budget north of Holland, Michigan. . . . .	53
27 Historical shorelines immediately south of Holland, Michigan, between 1849 and 1945 . . . . .	54
28 Historical shorelines farther south of Holland, Michigan, between 1871 and 1945 . . . . .	55
29 Computed data versus actual data . . . . .	60

CONVERSION FACTORS, U.S. CUSTOMARY TO METRIC (SI) UNITS OF MEASUREMENT

U.S. customary units of measurement used in this report can be converted to metric (SI) units as follows:

Multiply	by	To obtain
inches	25.4	millimeters
	2.54	centimeters
square inches	6.452	square centimeters
cubic inches	16.39	cubic centimeters
feet	30.48	centimeters
	0.3048	meters
square feet	0.0929	square meters
cubic feet	0.0283	cubic meters
yards	0.9144	meters
square yards	0.836	square meters
cubic yards	0.7646	cubic meters
miles	1.6093	kilometers
square miles	259.0	hectares
knots	1.852	kilometers per hour
acres	0.4047	hectares
foot-pounds	1.3558	newton meters
millibars	$1.0197 \times 10^{-3}$	kilograms per square centimeter
ounces	28.35	grams
pounds	453.6	grams
	0.4536	kilograms
ton, long	1.0160	metric tons
ton, short	0.9072	metric tons
degrees (angle)	0.01745	radians
Fahrenheit degrees	5/9	Celsius degrees or Kelvins <sup>1</sup>

<sup>1</sup>To obtain Celsius (C) temperature readings from Fahrenheit (F) readings, use formula:  $C = (5/9) (F - 32)$ .

To obtain Kelvin (K) readings, use formula:  $K = (5/9) (F - 32) + 273.15$ .



## SYMBOLS AND DEFINITIONS

a	proportionality constant ( $\beta = \alpha\alpha$ )
B	height of bluff (in case of erosion) or berm (in case of accretion)
$C_b$	phase velocity at breaking
$C_o$	deepwater phase velocity
$D_c$	water depth at $y_c$
d	water depth
$d_b$	breaking depth
$dV_1$	variation of sand volume due to horizontal displacement during time, dt
$dV_2$	variation of sand volume due to beach slope variation during time, dt
$G_b$	group velocity at breaking
$G_o$	deepwater wave group velocity
g	gravity acceleration
$H_b$	breaking wave height
$H_o$	deepwater wave height
$K_D$	diffraction coefficient
$K_R$	refraction coefficient from deep water to the line of breaking inception
$K_s$	percentage of silt
k	time-constant parameter
$L_b$	wavelength at breaking
$L_o$	deepwater wavelength
l	length of groin perpendicular to shore
M	loss of sand by rip currents
m	beach slope at shoreline
ox	horizontal axis parallel to the average initial beach profile
oy	horizontal axis perpendicular to x, oriented positively seaward
oz	vertical axis, positive upward
$P_l$	longshore energy flux
Q	dimensionless littoral drift discharge
$Q_s$	littoral drift discharge in cubic yards per year
$Q_{yf}$	loss of bluff volume (in case of erosion) due to silt
$Q_{ys}$	loss of bluff volume (in case of erosion) due to silt

SYMBOLS AND DEFINITIONS--Continued

$Q_{yw}$	loss of sand by wind
$q_y$	sand discharge in a direction perpendicular to the beach
S	average bottom slope to depth of no motion
$S_y$	horizontal displacement at depth, $D_c$ , characterizing slope variation
s	shoreline
T	wave period
t	time
V	volume of sand over a stretch of shoreline, $\Delta x$ , unity
$x_s, y_s$	shoreline coordinates
y	dimensionless shoreline
$y_c$	deepwater limit of the beach
$z_b$	function of x, y, t defining the bottom topography
$z_s$	shoreline elevation above a datum $z = 0$
A	$7.5 \times 10^3 \frac{g^2}{64} \times T$
$\alpha$	deepwater wave angle with the ox-axis
$\alpha_b$	angle of breaking with the shoreline
$\alpha_o$	deepwater wave angle with the shoreline
$\beta$	angle of the beach limit with the ox-axis in front of a groin
$\Delta y_o$	horizontal displacement of the beach profile during time, dt
$\Delta y_1$	function characterizing beach-slope variation as function of x
$\Delta y_2$	function characterizing beach-slope variation as function of t
$\Delta y_2'$	function characterizing beach-slope variation with time due to rapid change of sea level
$\Delta y_2''$	function characterizing beach-slope variation with time due to manmade structures such as groin or navigation works
$\Delta y_{2m}''$	a symptotic (in axium) value of $\Delta y_2''$ when $t \rightarrow \infty$
$\theta$	variation of wave direction by diffraction
$\theta'$	angle of wave ray with a perpendicular to shore in a diffraction zone
$\rho$	water density

# A NUMERICAL MODEL FOR PREDICTING SHORELINE CHANGES

*by*  
*Bernard Le Mehaute and Mills Soldate*

## I. INTRODUCTION

This report establishes a mathematical model for shoreline evolution and calibrates the model with a test case at Holland Harbor, Michigan. Even though the mathematical model is general and could be applied to a number of situations, the emphasis is on the Great Lakes, and more specifically, on shoreline evolution near navigation structures.

An interim report by Le Mehaute and Soldate (1977) reported on the feasibility of applying existing mathematical models to real case situations. This report is a continuation of that first investigation.

The present mathematical model includes many of the characteristics already covered in the literature. In addition, the model presents an integrated approach on a large number of phenomena previously neglected. Its main purpose is to develop a practical numerical scheme which could be used to predict shoreline evolution. The model would then be able to point out the shortcomings in the present state of knowledge. Therefore, the mathematical model covers some aspects of shoreline evolution which cannot be quantified with the data obtained from the considered test case of Holland Harbor. The mathematical model then has to be regarded as a research guide for the future.

One important aspect is the effect of sand size and density. It is well known that the rate of shoreline erosion and sediment loss is largely affected by these parameters. The fine sand is transported offshore, while larger size sand tends to proceed alongshore according to a littoral drift formula. This effect could not presently be quantified; therefore, it is introduced in the mathematical model as a constant.

The present mathematical model can continuously be upgraded as the state-of-the-art progresses, and as the model is tested for a large number of cases. It is important to remember that the model deals with long-term shoreline evolution as defined in Le Mehaute and Soldate (1977). Short-term evolution must be considered as local perturbations which are superimposed on the presently defined topography.

Three time scales of shoreline evolution which can be distinguished are (a) geological evolution over hundreds and thousands of years, (b) long-term evolution from year-to-year or decade, and (c) short-term or seasonal evolution during a major storm.

Associated with these time scales are distances or ranges of influence over which changes occur. The geological time scale deals, for instance, with the entire area of the Great Lakes. The long-term evolution deals with a more limited stretch of shoreline and range of influence; e.g., between two headlands or between two harbor entrances. The short-term evolution deals with the intricacies of the surf zone circulation; e.g., summer-winter profiles, bar, rhythmic beach patterns, etc.

For the problem under consideration, long-term evolution is of primary importance, the short-term evolution appearing as a superimposed perturbation on the general beach profile. Evolution of the coastline is characterized by low monotone variations or trends on which are superimposed short bursts of rapid development associated with storms.

The primary cause of long-term evolution is water waves or wave-generated currents. Three phenomena intervene in the action which waves have on shoreline evolution:

- (a) Erosion of beach material by short-period seas versus accretion by longer period swells;
- (b) effect of water level changes on erosion; and
- (c) effect of breakwaters, groins, and other structures.

Although mathematical modeling of shoreline evolution has inspired some research, it has received only limited attention from practicing engineers. The present methodology is based mainly on (a) the local experience of engineers who have a knowledge of their sectors, understand littoral processes, and have an inherent intuition of what should happen; and (b) movable-bed scale models that require extensive field data for their calibration.

In the past, theorists have been dealing with idealized situations, rarely encountered in engineering practice. Mathematical modelers apparently have long been discouraged by the inherent complexity of the phenomena encountered in coastal morphology. The lack of well-accepted laws of sediment transport, offshore-onshore movement, and poor wave climate statistics have made the task of calibrating mathematical models very difficult. Considering the importance of determining the effect of construction of long groins and navigation structures, and the progress made in determining wave climate and littoral drift, a mathematical approach now appears feasible.

The complexity of beach phenomena could, to a large extent, be taken into account by a numerical mathematical scheme (instead of closed-form solutions), dividing space and time intervals into small elements in which the inherent complexity of the morphology could be taken into account. Furthermore, better knowledge of the wave climate, a necessary input, will allow a better calibration of coastal constants (such as those in the littoral drift formula).

In past investigations (Le Mehaute and Soldate, 1977), many important effects have been neglected, such as combined effects of wave diffraction around littoral obstacles, change of sea level, height of berm and bluff, beach slope, etc. The present investigation attempts to include all the important factors associated with long-term shoreline evolution. In the case of the Great Lakes, importance must be given to variations in lake level. The coastal zone is defined by a three-dimensional bottom topography instead of a two-dimensional shoreline (or two lines) as in the previous cases.

Mathematical modeling is essentially approached by:

- (a) Understanding the phenomenology of shoreline evolution quantitatively.

(b) Calibrating, determining empirical constants, and separating various effects, such as due to change of lake level, navigation structures, etc.

(c) Predicting long-term future evolution.

(d) Assessing the effect of future construction.

The mathematical model presented in this report is just a first step in this direction. Much of the model may be modified after the application of the mathematical model to other cases which could be used for further calibration.

Theoretical developments for the model are presented in Section II. Section III describes the shoreline evolution recorded at Holland Harbor, Michigan, and compares the mathematical model with the test case investigated. Section IV provides recommendations and conclusions. An Appendix describes a computer program to investigate shoreline behavior.

## II. THEORETICAL DEVELOPMENTS

Consideration is given to a coastal zone limited by boundaries at a small distance from the surf zone (Fig. 1). The bottom topography is defined in a three-coordinate system,  $oxyz$ , by a function  $z_b = f(x,y,t)$  where the  $ox$ -axis is parallel to the average shoreline direction, the  $oy$ -axis is perpendicular seaward, and  $oz$  is positive upward from a fixed horizontal datum. The angle of the shoreline with the  $ox$ -axis is small. The shoreline is defined by  $y = y_s$ ,  $z = z_s = z_b(x, y_s, t)$  which also defines the sea level as a function of time.

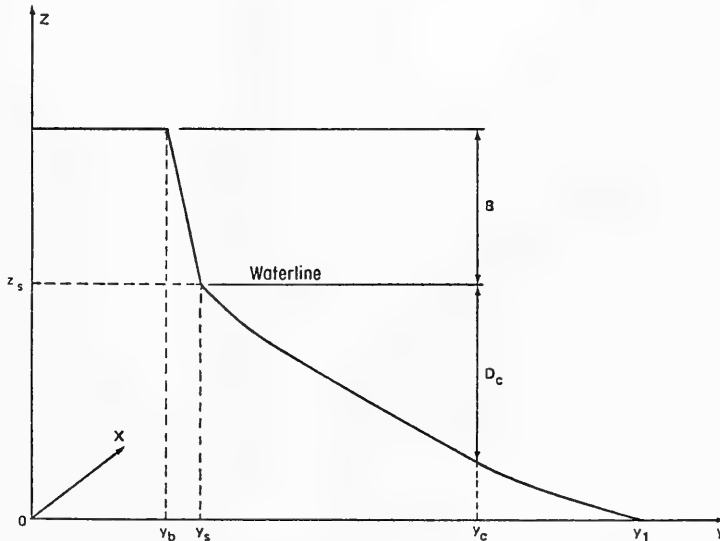


Figure 1. Coastal zone.

The deepwater limit of the beach is  $y = y_c$ . (This limit defines the contour line where the sand is no longer moved by wave action.) The water depth at  $y = y_c$  is  $D_c$ . It will be assumed that  $D_c$  remains constant as sea level and beach profiles change. Therefore,  $\partial z_s / \partial t = \partial z_c / \partial t$ .

$B$  is the height of the bluff in case of erosion, i.e., when  $\partial y_s / \partial t < 0$ , and the height of the berm in case of accretion, i.e., when  $\partial y_s / \partial t > 0$  (Fig. 2).

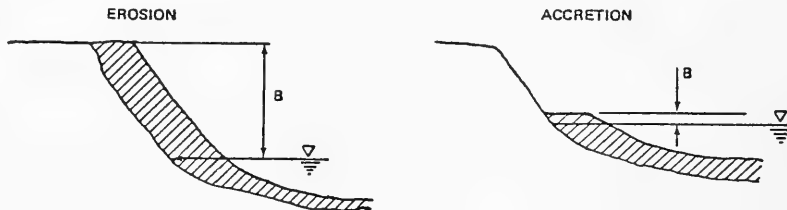


Figure 2. Height of bluff or berm.

The quantity of sand over a stretch of shoreline,  $\Delta x = \text{unity}$  and bounded by the datum,  $z = 0$ ,  $y = 0$ , and the beach profile  $z_b$  at time,  $t$ , is

$$V(t) = \int_0^{y_1} z_b(x, y, t) dy.$$

Assume that, for some reason, the beach profile changes during an infinitesimal amount of time,  $dt$ . A further assumption is that the initial beach profile which is considered at time,  $t = t_i$ , could be the normal "equilibrium profile." (The equilibrium profile may never exist under varying prototype conditions (similarly two-dimensional waves never exist), but it is a convenient idealized concept which could be approached in two-dimensional wave tank experiments. In this case, it could be defined as the statistical long-term average beach profile which exists under a given wave climate. The model here is actually independent from this definition.)

The departure and modification from this initial beach profile can be characterized by (see Fig. 3):

(a) A translation in the  $yz$  plane defined by an elementary vector of components.

$$\frac{\partial y_s}{\partial t}, \frac{dD}{dt}$$

where  $dD/dt$  is the rate of change of sea level. Note that this translation is independent from the beach profile and, in particular, if the beach profile normally exhibits a number of significant bar formations, under normal conditions the translation will reproduce this characteristic at the same water depth.

(b) A perturbation characterizing the departure or variation from the initial profile. Since the rate of the vertical component

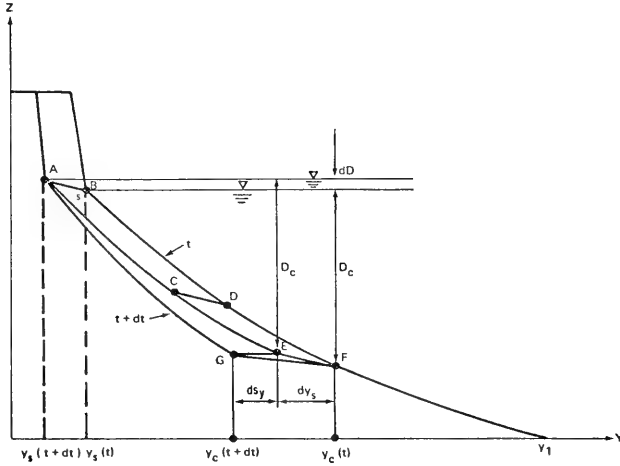


Figure 3. Change of beach profile.

of translation is  $dD/dt$ , the perturbation can be defined only by a horizontal displacement. At the deepwater limit,  $D_c$ , the horizontal displacement characterizing the rate of change of the average beach slope is defined by

$$\frac{\partial S_y(x, t)}{\partial t}$$

so that

$$\frac{\partial y_c}{\partial t} = \frac{\partial y_s}{\partial t} + \frac{\partial S_y}{\partial t}$$

The quantity of sand within the considered domain at time  $(t + dt)$  is

$$V(t + dt) = \int_0^{y_1} z_b(x, y, t + dt) dy \quad (1)$$

and the variation

$$\frac{dV}{dt} = \int_0^{y_1} \frac{dz_b}{dt} dy \quad (y_1 \text{ and } 0 \text{ are fixed limits})$$

i.e.,

$$\frac{dV}{dt} = \int_0^{y_1} \left( \frac{\partial z_b}{\partial t} + \frac{\partial z_b}{\partial y} \frac{dy}{dt} + \frac{\partial z_b}{\partial x} \frac{dx}{dt} \right) dy$$

where  $\partial z_b / \partial x$  is the variation of beach elevation along the  $ox$ -axis. Since the angle of the beach with the  $ox$ -axis is small

$$\frac{\partial z_b}{\partial x} \ll \frac{\partial z_b}{\partial y}; \left( \frac{\partial z_b}{\partial y} = m \text{ is the beach slope} \right),$$

i.e., the change in  $z$  occurring along the beach is small relative to change across profile and the beach profile variation over a distance  $dx$  is small but remains an infinitesimal of higher order than over a distance  $dy$ .

For the same reason, the velocity of beach variation along the  $ox$ -axis  $dx/dt$  is small as compared to the beach variation along  $oy$ ; therefore

$$\frac{\partial z_b}{\partial x} \frac{dx}{dt} \ll \frac{\partial z_b}{\partial y} \frac{dy}{dt}$$

and could be neglected. To evaluate the other terms it is simpler to refer to Figure 3. It is seen that the integral is equal to the sum of:

(a) The change of volume of sand,  $dv/dt$ , due to the translation,  $\partial y_s/\partial t$ , is the sum of the change of volume due to the horizontal translation (Fig. 4)

$$(B + C) \frac{\partial y_s}{\partial t} \quad (2)$$

and the change of volume due to the vertical displacement

$$(y_c - y_b) \frac{dD}{dt} \quad (3)$$

where  $y_b$  is the ordinate characterizing the location of the bluff.

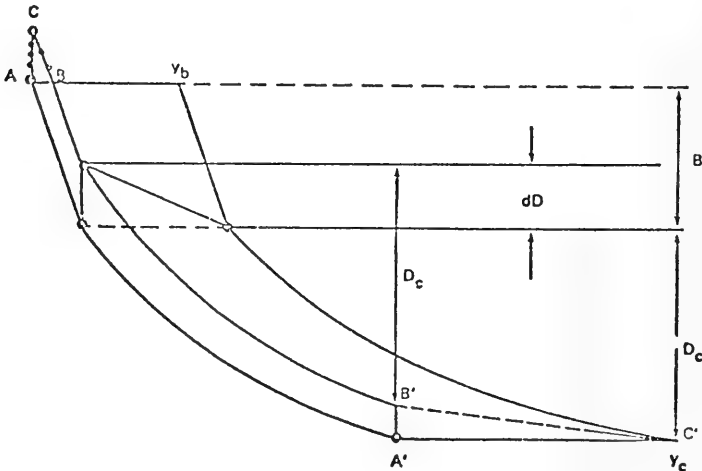


Figure 4. Changes of sand volume due to translation of one beach profile.



The sea level displacement,  $dD$ , being small, the difference in the quantity of sand represented by the two triangles ABC and A'B'C' in Figure 4 is considered as a difference of infinitesimals and therefore is neglected. So, combining equations (2) and (3)

$$\frac{dV}{dt} = (B + D_e) \frac{\partial y_s}{\partial t} - (y_e - y_b) \frac{dD}{dt} \quad (4)$$

It is seen that when  $dV/dt = 0$

$$dy_s = \frac{y_e - y_b}{B + D} dD = \frac{dD}{S}$$

where  $S$  is the average bottom slope. Note that this expression is independent of the beach profile and, therefore, implicitly takes into account bar formation.

(b) The change of volume due to the perturbation and departure from the equilibrium profile. This departure is characterized by a change of slope. Therefore, the corresponding variation of sand volume (area AEG in Fig. 3) is

$$\frac{dV_2}{dt} = \frac{1}{2} D_e \frac{dS_y}{dt} \cong \frac{1}{2} D_e \frac{\partial S_y}{\partial t} \quad (5)$$

in accordance with the previous assumption. Therefore, the total variation of sand volume,  $dV/dt$ , is (adding eqs. 4 and 5):

$$\frac{dV}{dt} = (B + D_e) \frac{\partial y_s}{\partial t} - (y_e - y_b) \frac{dD}{dt} + \frac{1}{2} D_e \frac{\partial S_y}{\partial t} \quad (6)$$

This variation of volume is due to the variation of littoral drift along the ox-axis and the onshore-offshore motion. The following terms are included:

(a) The discharge of sand leaving the beach per unit of width includes:

(1)  $Q_{yw}$  due to loss of sand by wind.

(2)  $Q_{ys}(x)$  due to the quantity of silt contained in the bluff and which tends to move offshore by suspension. This loss occurs only in case of erosion ( $\partial y_s/\partial t < 0$ ) and is equal to  $Q_{ys} = K_s B \partial y_s/\partial t$ , where  $K_s$  is the percentage of silt in the bluff.

(3)  $Q_{yf}$  due to the loss of sand from the beach by density current during a storm.  $Q_{yf}$  is a function of the size distribution and density of material. A beach of fine material ( $< 0.1 \text{ mm}$ ) tends to erode more rapidly than a beach of coarse material ( $> 1 \text{ mm}$ ). The coarse material tends to move along the shore while the fine sand moves offshore.

The determination of these three quantities is given from sand budget investigations.

(b) A general term,  $M(x,t)$ , expressing the local variation in the sand budget due to loss of sand by rip currents along groins, and to sudden dumping of sand in case of beach nourishment or flood.

(c) The variation of littoral drift along the ox-axis which is

$$Q_S(s) - Q_S(x + dx) = - \frac{\partial Q_S}{\partial x} dx \quad (7)$$

Many formulas in literature sources express the rate of longshore transport,  $Q_S$ , as a function of the incident wave energy along a straight shoreline. Longshore transport is also a function of the sand characteristics (size distribution and density), wave steepness, beach slope, etc.

The form of this formulation on shoreline evolution is of paramount importance. In particular, determination of the relative rate of sediment transported in suspension and by bedload is very important since this ratio influences the loss of sediment by rip currents.

Such evaluation is beyond the state-of-the-art, and any improvement would require a major effort beyond the scope of the present investigation. Any improvement in the longshore transport rate formula could eventually be introduced in the model at a later date. Therefore, it is assumed that the rate of sediment transport is independent of density and size and depends solely on the longshore energy flux,  $P_\ell$ , by the empirical relationship

$$Q_S = 7.5 \times 10^3 P_\ell \quad (8)$$

where  $Q_S$  is in cubic yards per year.

$P_\ell$  is in foot-pounds per second per foot of shoreline and is expressed by the relationship (U.S. Army, Corps of Engineers, Coastal Engineering Research Center, 1977)

$$P_\ell = \frac{\rho g^2}{64\pi} T(H_0 K_R)^2 \sin 2\alpha_b \quad (9)$$

where

$K_R$  = refraction coefficient from deep water to the line of breaking inception

$T$  = wave period

$H_0$  = deepwater wave height

$\alpha_0$  = angle of the deepwater wave with the shoreline

$\alpha_b$  = angle of breaking with the shoreline

Note that this equation expresses implicitly the rate of littoral drift along a straight shoreline in terms of breaking wave characteristics (except for the deepwater wave height,  $H_0$ ). The equation is assumed to hold in case

of gentle beach curvature. The refraction coefficient,  $K_R$ , and angle,  $\alpha_b$ , can be determined as functions of the deepwater wave characteristics  $H_0$ ,  $T$ ,  $\alpha_0$  (or  $\alpha_b$ ) and the angle of the shoreline at breaking,  $\partial y_s / \partial x$ .

In the case of a groin perpendicular to the shore, at  $x \rightarrow -\infty$ , the deep-water wave angle,  $\alpha_0$ , with bottom contours is equal to the angle  $\alpha$  of the wave with the  $ox$ -axis since the shoreline has the same direction as the  $ox$ -axis; at  $x = 0$  (i.e., at the groin), the shoreline becomes parallel to the incident wave crest very rapidly. Therefore,  $\alpha_0 = 0$  and

$$\alpha_0 = -\tan^{-1} \left. \frac{\partial y_s}{\partial x} \right|_{x=0} \quad (10)$$

In the general case, for any value of  $x$

$$\alpha_0 = \alpha + \tan^{-1} \frac{\partial y_s}{\partial x} \quad (11)$$

The breaking wave characteristics of wave height,  $H_b$ , water depth  $d_b$ , and the angle of breaking  $\alpha_b$  can be obtained from the deepwater wave characteristics,  $H_0$ ,  $T$ , and  $\alpha_0$ .  $\alpha_0$  is given by equation (11) in terms of  $\alpha$  and  $\partial y_s / \partial x$  which takes into account the curvature of the shoreline. The following equations permit a determination of  $H_b$ ,  $d_b$ , and  $\alpha_b$ , provided the bottom contours are parallel along a wave ray (Le Mehaute, 1961), but could be curved along the shoreline (Fig. 5):

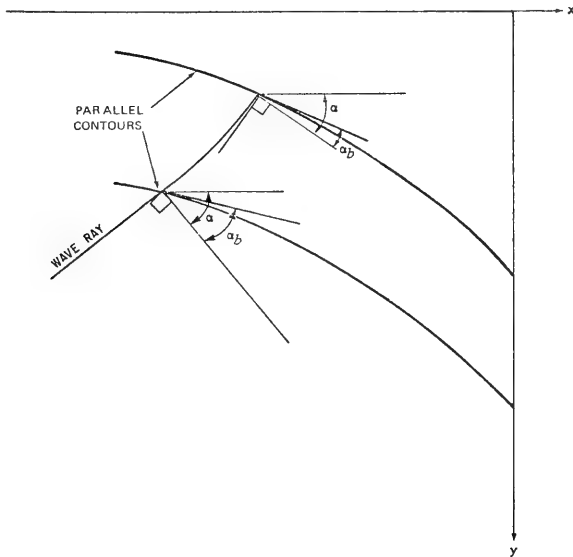


Figure 5. Effects of wave refractions on a curved beach.

(a) Snell's law.

$$\frac{C_b}{C_o} = \frac{\sin \alpha_b}{\sin \alpha} = \frac{\sqrt{gd_b}}{gT/2\pi} \quad (12)$$

(b) Wavelength (dispersion relation).

$$\frac{L_b}{L_o} = \tan h \left( \frac{2\pi d_b}{L_b} \right) \quad (13)$$

(c) Conservation of energy flux between wave orthogonals (G is the group velocity).

$$H_o^2 \cos \alpha_o G_o = H_b^2 \cos \alpha_b G_b \quad (14)$$

(d) Breaking criteria.

$$\frac{H_b}{L_b} = 0.14 \tan h \frac{2\pi d_b}{L_b} \quad (15)$$

From these equations, it has been shown (Le Mehaute and Koh, 1967) that when  $\alpha_o$  remains smaller than  $50^\circ$ ,  $\alpha_b$  could be approximated as

$$\alpha_b \cong \alpha_o \left( 0.25 + 5.5 \frac{H_o}{L_o} \right) \quad (16)$$

where

$$L_o = \frac{gT^2}{2\pi}$$

Therefore, the refraction coefficient

$$K_R = \left( \frac{\cos \alpha_o}{\cos \alpha_b} \right)^{1/2}$$

could be written, inserting  $\alpha_o$  as given by equation (11), and  $\alpha_b$  as given by equation (16)

$$K_R = \left( \frac{\cos \left( \alpha - \tan^{-1} \frac{\partial y_s}{\partial x} \right)}{\cos \left[ \left( \alpha - \tan^{-1} \frac{\partial y_s}{\partial x} \right) \left( 0.25 + 5.5 \frac{2\pi H_o^2}{gT^2} \right) \right]} \right)^{1/2} \quad (17)$$

Now it is possible to formulate the variation of littoral drift over a distance  $\Delta x = \text{unity}$ . From equation (9)

$$\frac{\partial Q_s}{\partial x} = AH_o^2 K_R^2 2 \cos 2\alpha_b \frac{\partial \alpha_b}{\partial x} + AH_o^2 2K_R \frac{\partial K_R}{\partial x} \sin 2\alpha_b \quad (18)$$

where

$$A = 7.5 \times 10^3 \frac{\rho g^2}{\sigma + \pi} T$$

On the other hand, since (see eq. 16)

$$\frac{\partial \alpha_b}{\partial x} = \frac{\partial \alpha_o}{\partial x} \left( 0.25 + 5.5 \frac{H_o}{L_o} \right) \quad (19)$$

and by taking into account equation (11)

$$\frac{\partial \alpha_c}{\partial x} = \frac{1}{1 + \left( \partial y_s / \partial x \right)^2} \frac{\partial^2 y_s}{\partial x^2} \quad (20)$$

Finally, by inserting equation (20) into equation (19)

$$\frac{\partial \alpha_b}{\partial x} = \frac{0.25 + 5.5 \frac{H_o}{L_o}}{1 + \left( \partial y_s / \partial x \right)^2} \frac{\partial^2 y_s}{\partial x^2} \quad (21)$$

In case of wave diffraction, the wave height varies significantly along a wave crest. Then, the previous refraction coefficient,  $K_R$ , has to be replaced by a combined diffraction-refraction coefficient, such as  $K_D K_R$ . (A diffraction current in opposite direction to a longshore current takes place at a distance from the end of the groin.) The variation  $\partial K_D / \partial x$  is much larger than  $\partial K_R / \partial x$ . Therefore, in analogy with equation (18)

$$\frac{\partial Q_S}{\partial x} = AH_o^2 K_R^2 \left( 2K_D^2 \cos 2\alpha_b \frac{\partial \alpha_b}{\partial x} + 2K_D \frac{\partial K_D}{\partial x} \sin 2\alpha_b \right) \quad (22)$$

In a diffraction zone,  $\alpha_b$  is due to the sum of variation of shoreline direction,  $\tan^{-1} \partial y_s / \partial x$ , and because of diffraction the rotation of the wave crest around the end of the groin,  $\theta$  (Fig. 6).  $\theta$  is the angle which has the end of the groin as apex and extends from the limit of the shaded area to the considered location defined by  $x$ . Figure 6 shows that  $\theta = \alpha_o - \theta'$  and  $\theta' = \tan^{-1} x/\ell$ , where  $\ell$  is the length of the groin. Therefore,

$$\alpha_b \cong \tan^{-1} \frac{\partial y_s}{\partial x} + \alpha_o - \tan^{-1} \frac{x}{\ell}, \quad (23)$$

$$- \frac{\partial \theta}{\partial x} = \frac{\partial \theta'}{\partial x} = \frac{1}{\ell} \frac{1}{1 + \left( x/\ell \right)^2} \quad (24)$$

and, differentiation equation (23) and inserting equation (24)

$$\frac{\partial \alpha_b}{\partial x} = \frac{1}{1 + \left( \partial y_s / \partial x \right)^2} \frac{\partial^2 y_s}{\partial x^2} + \frac{1}{\ell} \frac{1}{1 + \left( x/\ell \right)^2} \quad (25)$$

where  $\partial K_D / \partial x$  is the coefficient of variation of wave height due to combined effects of wave diffraction and wave refraction. It also includes the effect of diffraction current.

An empirical formulation for determining the combined effect of diffraction and refraction is more suitable to quantitative analysis of a real sea spectrum

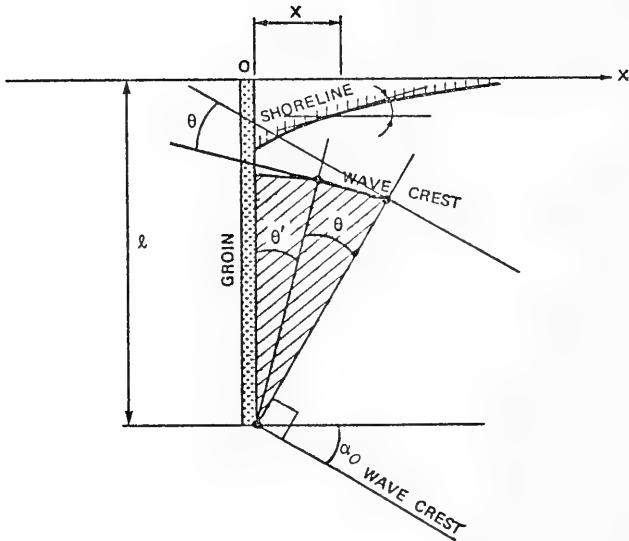


Figure 6. Diffraction zone notation.

than more exact theories of wave diffraction which are valid for periodic waves over a horizontal bottom and are represented by a Fresnel integral. For this, it will be assumed that the energy travels laterally along a wave crest as well as along a wave ray. The lateral speed of propagation is assumed to be equal to the group velocity of a periodic wave of average period. (Actually, since the problem is confined to very shallow-water waves, and the longest waves of the spectrum diffract most, the limit of the diffraction zone is defined by an angle such as the velocity of propagation of wave energy along the crest and is simply  $\sqrt{gD}$ , where  $D$  is the water depth.) This lateral transmission of energy results in a decrease of wave energy from the exposed area to the shaded area, such that (Fig. 7)

$$\int_A^C H^2 dx = \int_0^D H_0^2 ds \quad (26)$$

where  $s$  is the distance along a crest from the end of the groin. Figure 7 shows from simple geometrical relationships that

$$\begin{aligned} OD &= \frac{l}{\cos(\alpha_0 + 45^\circ)} \frac{\sqrt{2}}{2} \\ oA &= -l \tan(45^\circ - \alpha_0) \\ oC &= l \tan(45^\circ + \alpha_0) \end{aligned} \quad (27)$$

therefore,

$$H_0^2 \frac{l}{\cos(\alpha_0 + 45^\circ)} \frac{\sqrt{2}}{2} = \int_{-l \tan(45^\circ - \alpha_0)}^{l \tan(45^\circ + \alpha_0)} H^2 dx \quad (28)$$

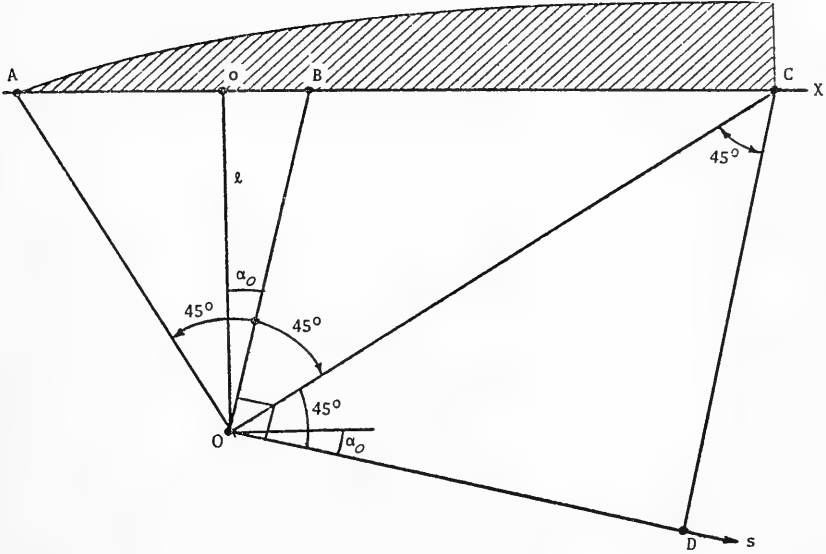


Figure 7. Notation for diffraction study.

In the case where the long groin is in the previously defined wave diffraction zone as in Figure 6, it is assumed that the wave energy which reaches the groin is absorbed by friction. It is also assumed that the combined effects of diffraction and refraction of a wave spectrum can simply be represented by a sinusoidal variation of wave height along the breaking line (Mobarek and Wiegell, 1966) (Fig. 7).

Assuming that  $K_D(x)$  is of the form  $\sin k(x - x_0)$  as shown in Figure 7, such as  $K_D$  at  $A = 0$ ,  $K_D$  at  $C = 1$ , then to satisfy these conditions

$$k = \frac{\pi}{2l} \left( \frac{1}{\tan(45^\circ - \alpha_0)} + \frac{1}{\tan(45^\circ + \alpha_0)} \right) \quad (29)$$

which after some simple trigonometric transformations can still be written

$$k = \frac{\pi}{4l} \cos 2\alpha_0 \quad (30)$$

to satisfy the equation expressing the conservation of energy flux, such as given by equation (29), then

$$a^2 = \frac{k^2 \sqrt{2l}}{\pi \cos(45^\circ + \alpha_0)} = \frac{\sqrt{2} \cos 2\alpha_0}{2 \sin \alpha_0}$$

and  $K_D(x) = H(x)/H_0$  is given by

$$K_D(x) = \left( \frac{\sqrt{2} \cos(2\alpha_0)}{2 \sin \alpha_0} \right)^{1/2} \sin \left( \frac{\pi \cos(2\alpha_0)}{4l} [x + l \tan(45^\circ - \alpha_0)] \right) \quad (31)$$

By differentiation equation (31)

$$\frac{dK_D(x)}{dx} = \left( \frac{\sqrt{2} \cos (2\alpha_o)}{2 \sin \alpha_o} \right)^{1/2} \frac{\pi \cos (2\alpha_o)}{4\ell} \cos \left( \frac{\pi \cos (2\alpha_o)}{4\ell} [x + \ell \tan (45^\circ - \alpha_o)] \right) \quad (32)$$

Inserting this value in the littoral drift equation (22) permits the mathematical model to be completed.

In summary, the variation of volume of sand  $dV/dt$  given by equation (6) is equal to the sum of:

(a) The loss of sand by wind  $Q_{yw}$ .

(b) The loss of silt  $Q_{ys} = K_s B \partial y_s / \partial t$  where  $K_s$  is the percentage of silt in the bluff.

(c) The loss of sand by density current during storm,  $Q_{yf}$ , and loss by rip current (or brought upon by nearby river).

(d) The quantity of sand dredged or (at the opposite) deposited during beach nourishment.

(e) The variation of littoral drift along the ox-axis is  $\partial Q_s / \partial x$ .

In a refraction zone alone,  $\partial Q_s / \partial x$  is given by equation (18) where  $K_r$  is given by equation (17).  $\alpha_b$  is given by equation (16) as a function of  $\alpha_o$ , and  $\alpha_o$  by equation (11), with respect to the ox-axis. Also,  $\partial \alpha_b / \partial x$  is given by equation (21).

In a diffraction zone  $\partial Q_s / \partial x$  is given by equation (22) instead of equation (18) and the diffraction coefficient  $K_D$  by equation (31), and  $\partial K_D / \partial x$  by equation (32) for a wave spectrum.  $\alpha_b$  is now given by equation (23) and  $\partial \alpha_b / \partial x$  by equation (25).

Since all the phenomenological equations have been established, it is more convenient to express them in dimensionless form. The "general" equation expressing the sand budget balance can still be written. (The loss terms have been dropped for simplicity and can easily be included if necessary.)

$$(B[x, t] + D_c) \frac{\partial y_s}{\partial t} + (y_c - y_b) \frac{dB}{dt} + \frac{1}{2} D_c \frac{d\Delta y}{dt} = \frac{\partial Q}{\partial x} \quad (33)$$

For an analysis, this equation is considered in dimensionless form. Let

$$\hat{L} = \frac{\text{length}}{B_o + D_c} \quad (34)$$

where  $B_o$  is chosen later

$$\hat{t} = \frac{At}{(B_o + D_c)^3} \quad (35)$$

$$Q = \frac{A}{2} K_R^2 K_D^2 \sin 2\alpha_b \quad (36)$$



The general equation is thus transformed to

$$\frac{B + D_e}{B_o + D_e} \frac{\partial \hat{y}_s}{\partial \hat{t}} + (\hat{y}_e - \hat{y}_b) \frac{d\hat{D}}{d\hat{t}} + \frac{1}{2} \frac{D_e}{B_o + D_e} \frac{d\Delta \hat{y}}{d\hat{t}} = \frac{\partial}{\partial \hat{x}} \frac{K_D^2 K_R^2 \sin 2\alpha_b}{2}$$

The hats will be dropped from all variables at this point in all discussions except those relating to observed results. Also, the subscript  $s$  for  $y$  and  $Q$  will be omitted. Hence, the general equation used in the following is

$$\frac{B + D_e}{B_o + D_e} \frac{\partial y}{\partial t} + (y_e - y_b) \frac{dD}{dt} + \frac{1}{2} \frac{D_e}{B_o + D_e} \frac{d\Delta y}{dt} = \frac{\partial}{\partial x} \frac{K_D^2 K_R^2 \sin 2\alpha_b}{2} \quad (37)$$

Recall

$$K_R^2 = \frac{\cos \alpha_o}{\cos \alpha_b}$$

where  $\alpha_o = \alpha + \tan^{-1} \partial y / \partial x$  and  $\alpha_b =$  function of  $\alpha_o$ , as  $f(\alpha_o)$  (the function  $f$  depends only on  $H_o/L_o$  as previously shown). Therefore,

$$\frac{1}{2} K_D^2 K_R^2 \sin 2\alpha_b = K_D^2 \cos \alpha_o \sin \alpha_b$$

Note

$$\frac{\partial}{\partial x} \cos \alpha_o \sin \alpha_b = \left( \cos \alpha_o \cos \alpha_b \frac{\partial f}{\partial \alpha_o} - \sin \alpha_o \sin \alpha_b \right) \frac{\partial \alpha_o}{\partial x} = F(\alpha_o) \frac{\partial \alpha_o}{\partial x}$$

The general equation (37) then becomes (after some rearrangements)

$$\frac{\partial y}{\partial t} = \frac{B_o + D_e}{B + D_e} F(\alpha_o) \frac{1}{1 + \left( \partial y / \partial x \right)^2} \frac{\partial^2 y}{\partial x^2} + R(x, y, t) \quad (38)$$

where

$$R(x, y, t) = \frac{B_o + D_e}{B + D_e} F(\alpha_o) \frac{\partial \alpha}{\partial x} - (y_e - y_b) \frac{dD}{dt} - \frac{1}{2} \frac{D_e}{B_o + D_e} \frac{d\Delta y}{dt} + 2K_D \frac{\partial K_D}{\partial x} \cos \alpha_o \sin \alpha_b \quad (39)$$

and

$$\alpha = \alpha(x) \text{ in the diffraction zone}$$

The above equation is the general dimensionless form which gives the time-dependent sand budget.

The general equation is nonlinear and appears to be impossible to solve analytically. As it is also difficult to solve computationally in the most universal case (where lake level, beach slope, and bluff-berm height vary as functions of  $x$ ,  $y$ ,  $t$ ), several simple cases are described in detail which indicate the behavior of the equations. Although numerical results are presented, detailed descriptions of the numerical methods used are given in a later discussion.

The simplest examples are those of beaches having negligible or identically constant bluff-berm, uniform beach slope, and uniform lake level. In these instances, the general equation (38) reduces to

$$\frac{\partial y}{\partial t} = F(\alpha_0) \frac{1}{1 + \left(\frac{\partial y}{\partial x}\right)^2} \frac{\partial^2 y}{\partial x^2} + 2K_D \frac{\partial K_D}{\partial x} \cos \alpha_0 \sin \alpha_D + F(\alpha_0) \frac{\partial \alpha}{\partial x} \quad (40)$$

subject to the appropriate boundary conditions.

Suppose (as shown in Fig. 8) the beach is initially zero, bounded by a breakwater which is a complete littoral barrier, and subjected to waves having uniform positive deepwater direction. The boundary conditions are

$$\frac{\partial y}{\partial x} = -\tan \alpha \quad \text{at } x = 0$$

$$\frac{\partial y}{\partial x} = 0 \quad \text{at } x = L$$

where  $L$  is a distance along  $ox$ , large enough so as not to be influenced by the groin.

The shoreline is calculated for a fixed  $H_0$ ,  $T$ , at intervals of equal  $\Delta t$  (shown in Fig. 8) for selected times. The general shape of these curves is similar to the type formulations obtained by Pelnard-Considere (1956).

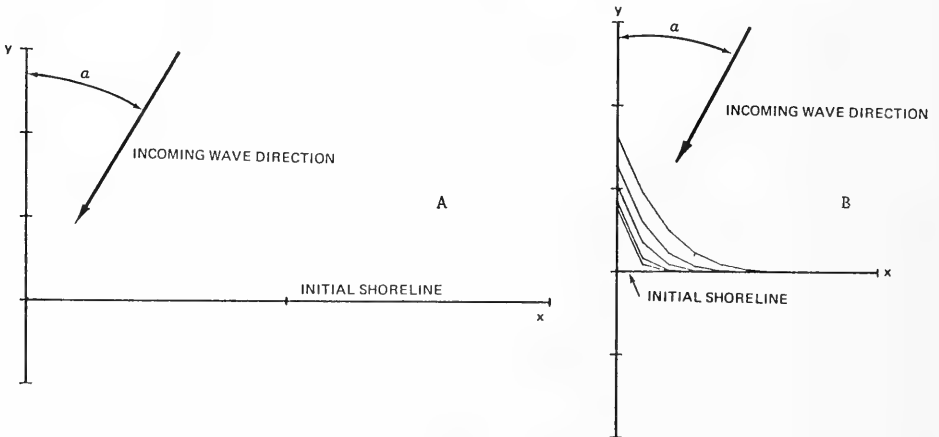


Figure 8. Initial shoreline and incoming wave direction (A); shorelines at successive times of  $1\Delta t$ ,  $2\Delta t$ ,  $5\Delta t$ ,  $10\Delta t$ , and  $20\Delta t$  (B) (vertical scale exaggerated).

An extension of the above example is shown in Figure 9 where both sides of a breakwater are considered. The initial position of the shoreline and wave conditions in deep water are as before (Fig. 9). The boundary conditions become

$$\frac{\partial y}{\partial x} = 0 \quad \text{at} \quad x = -L$$

$$\frac{\partial y}{\partial x} = 0 \quad \text{at} \quad x = -0 \quad (\text{simplification of more exact condition})$$

$$\frac{\partial y}{\partial x} = -\tan \alpha \quad \text{at} \quad x = +0$$

$$\frac{\partial y}{\partial x} = 0 \quad \text{at} \quad x = +L$$

The uniform depth theory of Penny and Price (1952) is used as an approximation (not substantiated) for diffraction about the end of the breakwater. The shoreline is calculated for various multiples of a fixed  $\Delta t$  (Fig. 9,A).

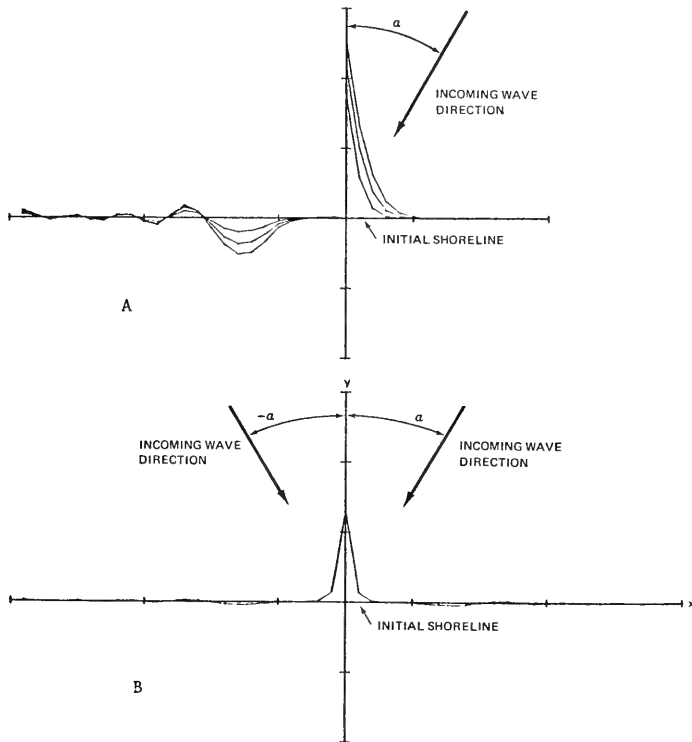


Figure 9. Shorelines at successive times of  $5\Delta t$ ,  $10\Delta t$ , and  $15\Delta t$  (A); shorelines for time  $2\Delta t$  (B) (vertical scale exaggerated).

Allowing the wave direction to alternate between  $+\alpha$  and  $-\alpha$  at a fixed rate gives an interesting variant to the previous example. The boundary conditions are as before for  $\alpha > 0$ . The results are shown in Figure 9(B) for the same values as the physical parameters used in the problem of Figure 9(A). Of interest is that the undulatory patterns of the shoreline in Figure 9(A) disappear in Figure 9(B). Hence, diffraction-induced undulations in a natural shoreline probably rarely appear since offshore wave climates are often multidirectional.

The numerical scheme used to generate the preceding examples was based on the use of implicit finite differences. Such schemes, whether implicit or explicit (or both), are commonly used to efficiently solve parabolic problems. However, even in the case where only refraction is considered (Fig. 8), the boundary condition

$$\frac{\partial y}{\partial x} = -\tan \alpha \quad \text{at } x = 0$$

numerically gives a solution which initially may not conserve mass, i.e., the integrated transport equation

$$\frac{\partial}{\partial t} \int_0^L y dx = Q(L)$$

may not be satisfied.

Unfortunately, this feature is unavoidable for most such schemes (the exceptions are discussed below) as the following demonstrates. Figure 10(A) shows an initially straight shoreline. In any finite-difference scheme, after one time increment  $\Delta t$ , the shoreline is bounded below by the solid shoreline in Figure 10(B). This shoreline has the least possible area,  $A$ , where

$$A = \frac{\Delta x^2}{2} \tan \alpha \quad (41)$$

The conservation of mass equations requires

$$\Delta t Q(L) = \Delta t \cos \alpha \sin \alpha_b \geq A$$

Thus,  $\Delta t$  must satisfy the inequality

$$\Delta t \geq \frac{1}{2} \frac{\sin \alpha}{\sin \alpha_b} \frac{\Delta x^2}{\cos^2 \alpha} \quad (42)$$

Since the accuracy (and in explicit schemes, stability as well) depends on the ratio  $\lambda = \Delta t / \Delta x^2$ , the above inequality places a lower bound on the accuracy of the solution which may be unacceptable in practice. The finite-difference form of the equation for the conservation of mass may be incorporated directly into the numerical scheme. In this case a solution exists which is similar to the previous case but shows a small erosion throughout the reach. For engineering applications, the primary quantity of interest is the amount of sand on a given shoreline. Then it is more important to conserve mass than to satisfy the shoreline boundary condition as written in the present form. The general equation is

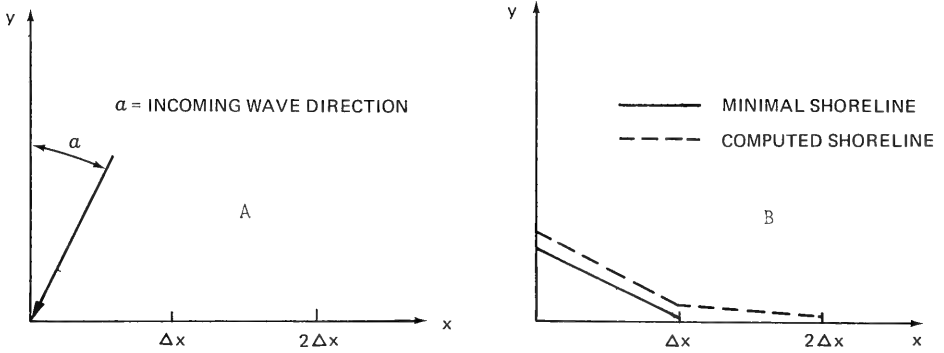


Figure 10. Initial shoreline and incoming wave direction (A); computed and minimal shorelines for finite-difference scheme of time  $1\Delta t$  (B).

now used to derive an equivalent equation for the transport  $Q$  which, although subject to similar numerical problems, will satisfy the transport boundary conditions exactly.

In a situation where only refraction is important, the general equation then becomes

$$\frac{\partial y}{\partial t} = \frac{\partial Q}{\partial x}$$

where  $Q$  is  $\cos \alpha_0 \sin \alpha_b$ ,  $\alpha_b$  is  $f(\alpha_0)$ , and  $\alpha_0$  is  $\alpha - \tan^{-1} \partial y / \partial x$ . Differentiating by  $x$  gives

$$\frac{\partial}{\partial t} \frac{\partial y}{\partial x} = \frac{\partial^2 Q}{\partial x^2} \quad (43)$$

The transport function  $Q$  can be considered as a function of  $\alpha_0$  which may be solved for  $\alpha_0$ , such as  $\alpha = g(Q)$ . Thus, the transport equation (43) becomes

$$\frac{\partial}{\partial t} \tan(\alpha_0 - \alpha) = \frac{\partial}{\partial t} \tan(g(Q) - \alpha) = \frac{\partial^2 Q}{\partial x^2}$$

therefore,

$$\frac{\partial g(Q)}{\partial t} = \cos^2 (g(Q) - \alpha) \frac{\partial^2 Q}{\partial x^2}$$

but

$$\frac{\partial g(Q)}{\partial t} = \frac{dg(Q)}{dQ} \frac{\partial Q}{\partial t}$$

therefore,

$$\frac{\partial Q}{\partial t} = \frac{\cos^2 (g(Q) - \alpha)}{dg(Q)/dQ} \frac{\partial^2 Q}{\partial x^2} \quad (44)$$

Assuming a solution for this equation is known, the shoreline  $y$  can be calculated from the equation

$$y(t,x) = y(0,x) + \int_0^t \frac{\partial Q}{\partial x} (t,x) dt$$

In practice, the equation for  $Q$  is not solved in the above form. Implicit in the above formulation is the assumption that the function  $g$  exists. However, as shown in Figure 11,  $g$  is not single-valued if the maximum range of the angle  $\alpha_0$  is greater than approximately  $41^\circ$ . This difficulty may be removed by considering the equation for  $Q$  and  $y$  as a system subject to the boundary conditions for  $Q$ . Note that

$$\frac{\cos^2 (g(Q) - \alpha)}{dg(Q)/dQ} = \frac{dQ}{d\alpha_0} \left/ \left[ 1 + \left( \frac{\partial y}{\partial x} \right)^2 \right] \right.$$

Hence, the equation for  $Q$  becomes

$$\frac{\partial Q}{\partial t} = \frac{dQ}{d\alpha_0} \frac{1}{1 + \left( \frac{\partial y}{\partial x} \right)^2} \frac{\partial^2 Q}{\partial x^2} \tag{45}$$

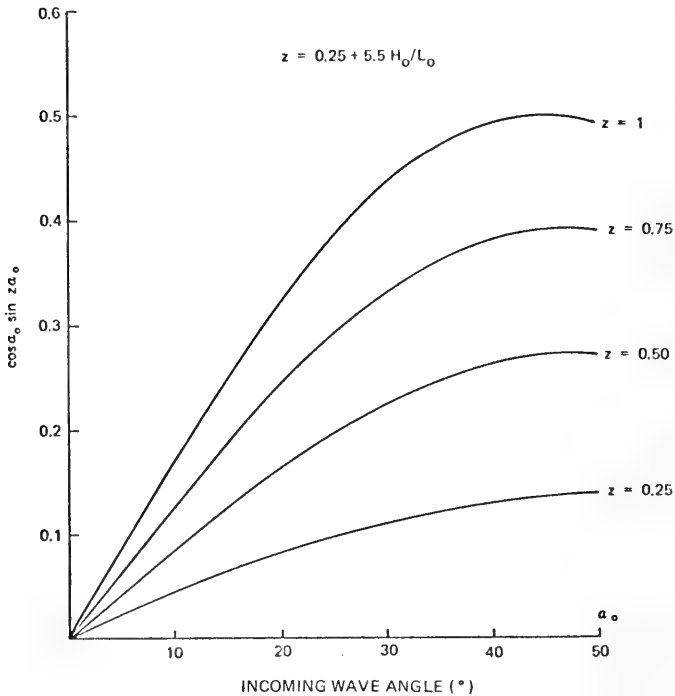


Figure 11. Transport function  $Q(\alpha_0) = \cos \alpha_0 \sin z\alpha_0$  for selected values of  $z$ .

This, together with the equation  $\partial y/\partial t = \partial Q/\partial x$ , is solved in a cyclic scheme. One possible method is the centered Crank-Nicolson type implicit-explicit scheme discussed below. Suppose  $y$  is given for all  $x$  at a given time,  $t$ , and that from  $t$  the wave climate is specified by the (constant) triple  $(\alpha, H_0, T)$ . Let

$$L(t, x) = \frac{dQ}{d\alpha_0} \frac{1}{1 + \left(\frac{\partial y}{\partial x}\right)^2}$$

$$\lambda = \frac{\Delta t}{\Delta x^2}$$

$L(t, x)$  = an approximation to  $L(t, x)$

Integrating the  $Q$  equation gives

$$Q(t + \Delta t, x) = Q(t, x) + \frac{\Delta t}{2} \left[ L(t, x) \frac{\partial^2 Q}{\partial x^2} \Big|_t + L(t + \Delta t, x) \frac{\partial^2 Q}{\partial x^2} \Big|_{t + \Delta t} \right] \quad (46)$$

where

$$\frac{\partial^2 Q}{\partial x^2} = \frac{Q(x + \Delta x) - 2Q(x) + Q(x - \Delta x)}{\Delta x^2} \quad (47)$$

Integrating the  $y$  gives

$$y(t + \Delta t, x) = y(t, x) + \frac{\Delta t}{2} \left[ \frac{\partial Q}{\partial x} \Big|_t + \frac{\partial Q}{\partial x} \Big|_{t + \Delta t} \right] \quad (48)$$

where

$$\frac{\partial Q}{\partial x} = \frac{Q(x + \Delta x) - Q(x - \Delta x)}{2\Delta x} \quad (49)$$

These equations are solved numerically, subject to the appropriate boundary conditions, in steps using the cyclic algorithm:

(a) Let  $\tilde{L}(t + \Delta t, x) = L(t, x) \forall x$ .

(b) Calculate  $Q(t + \Delta t, x) \forall x$  subject to the appropriate boundary conditions.

(c) Calculate  $y(t + \Delta t, x) \forall x$ ; calculate  $L(t + \Delta t, x)$  and set this equal to  $\tilde{L}(t + \Delta t, x)$ ; then calculate new  $Q$ .

(d) If new  $Q$  compares with old  $Q$ , stop; if not go to step (c).

Tests with this scheme have shown that it converges to its limit after one application of step (c).

This method can easily be modified to solve the equation where both diffusion and variations in lake level are allowed; i.e.,  $m$  is the slope (refer to eqs. 37 to 40).

$$\frac{\partial y}{\partial t} = \frac{\partial}{\partial x} K_D^2 \cos \alpha_0 \sin \alpha_b - \frac{1}{m} \frac{dD}{dt} \quad (50)$$

For convenience, let  $Q = \cos \alpha_o \sin \alpha_b$

$$\tilde{Q} = K_D^2 Q \quad (51)$$

As before, referring to equations (43) and (44)

$$\frac{\partial}{\partial t} \frac{\partial y}{\partial x} = \frac{\partial}{\partial t} \tan (g(Q) - \alpha) = \frac{1}{\cos^2 (g(Q) - \alpha)} \frac{dg(Q)}{dQ} \frac{\partial Q}{\partial t} - \frac{1}{\cos^2 (g(Q) - \alpha)} \frac{\partial \alpha}{\partial t}$$

Also,

$$\frac{\partial \tilde{Q}}{\partial t} = K_D^2 \frac{\partial Q}{\partial t} + 2K_D \frac{\partial K_D}{\partial t} Q$$

from equation (51).

The second term in each of the above two equations is negligible in physical situations of usual interest where the distance between the shoreline and the tip of the breakwater is large compared to the distance the shoreline changes during a time  $\Delta t$ .

Therefore, the transport equation becomes

$$\frac{\partial \tilde{Q}}{\partial t} = \frac{K_D^2}{dg/\partial Q} \cos^2 (g(Q) - \alpha) \frac{\partial^2 \tilde{Q}}{\partial x^2} \quad (52)$$

and

$$\frac{\partial y}{\partial t} = \frac{\partial \tilde{Q}}{\partial x} - \frac{1}{m} \frac{dD}{dt} \quad (53)$$

This system is solved using the same type of algorithm as used previously.

In the present situation where only refraction is important, several approximations are possible which produce problems having analytic solutions. The most direct approximation, and essentially the assumption of Penard-Considere (1956), is to approximate

$$\frac{\partial y}{\partial t} = (z \cos \alpha_o \cos \alpha_b - \sin \alpha_o \sin \alpha_b) \frac{1}{1 + (\partial y / \partial x)^2} \frac{\partial^2 y}{\partial x^2} \quad (54)$$

where  $z = 0.25 + 5.5 H_o/L_o$  (see eq. 16), subject to the boundary conditions

$$\left. \frac{\partial y}{\partial x} \right|_{x=0} = -\tan \alpha$$

$$y(x,t) = 0 \text{ for } x = \infty$$

by

$$\frac{\partial y}{\partial t} = a \frac{\partial^2 y}{\partial x^2}$$



where  $a$  is a constant. For the standard breakwater problem, the most logical choice for this constant is given by

$$a = \frac{z}{1 + \tan^2 \alpha} = \left[ (z \cos \alpha_o \cos \alpha_b - \sin \alpha_o \sin \alpha_b) \frac{1}{1 + (\partial y / \partial x)^2} \right]_{x=0} \quad (55)$$

since the shoreline in this case is principally governed by its behavior at the breakwater. This problem (defined by eq. 55) has the solution

$$y(x,t) = 2 \tan \alpha \frac{\sqrt{at}}{\sqrt{\pi}} e^{-x^2/4at} - \tan \alpha x \operatorname{erfc} \left( \frac{x}{\sqrt{4at}} \right) \quad (56)$$

which is the same as that of Penard-Considere except that the constant  $a$  has been changed. This problem, however, doesn't conserve mass since

$$\frac{\partial}{\partial t} \int_0^{\infty} y(x,t) dx = z \sin \alpha \cos \alpha \sin \alpha \cos \alpha$$

When this approximation is used in the transport equation for  $Q$ , the problem becomes

$$\frac{\partial Q}{\partial t} = a \frac{\partial^2 Q}{\partial x^2}$$

subject to the boundary conditions

$$Q(x=0) = 0$$

$$Q(x=\infty) = \cos \alpha \sin \alpha_b$$

which has the solution

$$Q(x,t) = \cos \alpha \sin \alpha_b \operatorname{erf} \left( \frac{x}{\sqrt{4at}} \right) \quad (57)$$

Integrating the equation,

$$\frac{\partial y}{\partial t} = \frac{\partial Q}{\partial x}$$

gives

$$y(x,t) = \cos \alpha \sin \alpha_b \left[ \frac{\sqrt{2}}{\sqrt{\pi a}} t^{1/2} e^{-x^2/4at} - \frac{x}{a} \operatorname{erfc} \left( \frac{x}{\sqrt{4at}} \right) \right] \quad (58)$$

which is of the same form as the previous solution (eq. 56).

### III. INPUT DATA

#### 1. Description and History of Navigation Project at Holland Harbor.

The input data, which are pertinent only to the present investigation, deal exclusively with the area near Holland Harbor, Michigan (U.S. Army Engineer District, Detroit, 1975). Construction at Holland Harbor began about 1856 when the city of Holland cut through a narrow tongue of land between Lake Michigan and Lake Macatawa (Fig. 12). The present dimensions of the navigation project were established in 1909. The existing navigation structures have been constructed,

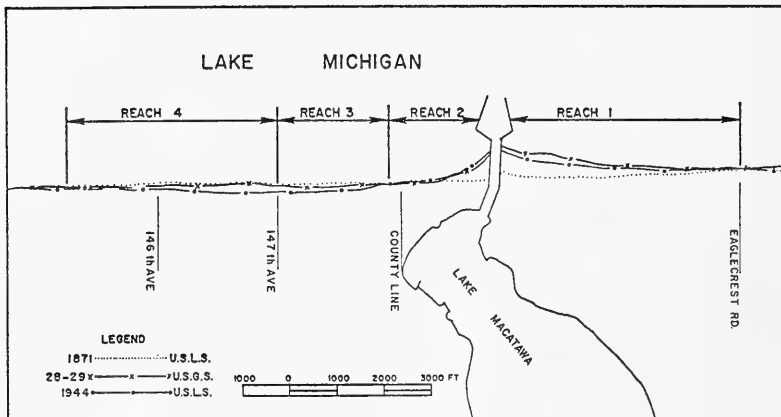


Figure 12. Layout of shoreline reaches characterized by different beach conditions.

reconstructed, and repaired by segments during different periods over the past 117 years. In general, the north side shows accretion while the south side shows accretion from the breakwater to about 1,200 feet south and then general erosion farther south.

The following areas (Fig. 12) appear to be affected by the navigation structures as evidenced by aerial photos, condition surveys, and plat maps for the period of record (1849 to 1945):

(a) North of Holland Harbor (Eaglecrest Road to the North Pier of Holland Harbor). It is considered that the accretion fillet north of the piers has been relatively stable since 1933. After that date, the predominantly southward-moving littoral drift has been diverted lake-ward resulting in rising nearshore elevations north of the breakwater and deposition of material in the entrance channel. This reach of shoreline, about 5,000 feet in length, is characterized by increasing accretion from north to south (Fig. 12, reach 1).

(b) South of Holland Harbor.

(1) Holland Harbor entrance channel to a point 200 feet south of the Ottawa-Allegan County line (Fig. 12, reach 2). Reach 2 extends about 2,000 feet south of Holland Harbor, and consists of a sand beach about 50 feet wide backed by low sand dunes. The shoreline adjacent to the south pier accreted at the rate of 9.6 feet per year from 1871 to 1944, a total of 700 feet. This area of accretion diminishes progressively southward from the piers to a point 200 feet south of the county line where the shoreline before major construction (1871) coincides with that of the 1929 and 1944 surveys.

(2) From 200 feet south of the Ottawa-Allegan County line to 147th Avenue (Fig. 12, reach 3). This reach is about 2,400 feet in length and is characterized by high, stabilized sand dunes (up to 120 feet above low water datum) which are being undercut by wave action.

(3) From 147th Avenue to a point approximately 1,900 feet south of 146th Avenue (Fig. 12, reach 4). Reach 4, about 4,500 feet long, is characterized by eroding sand dunes up to 225 feet high. Figure 12 shows that erosion is greater at the northern end of the reach and decreases progressively southward. At the southern end of the reach the shoreline before construction of the navigation structures coincides closely with that of the 1929 and 1944 surveys. Erosion appears to be greatest at a point about 800 feet south of 147th Avenue where the shoreline receded about 220 feet from 1866 to 1945, or an average of 3 feet per year.

The rates of movement of the shoreline near the harbor have decreased (1945-73) but the trends of accretion on the north side and erosion on the south side have continued. The present lower rates of shoreline movement are due to several factors:

(a) The rate of shoreline movement due to the navigation structures decreases with time.

(b) Local interests have built more shore protection structures as their property was threatened. The consequence of these structures is to reduce the apparent rate of erosion locally, but this is accomplished at the expense of steepening of the offshore bottom profiles and increased erosion downdrift. The shoreline protective structures now extend almost continuously from 1,000 feet to about 4,600 feet south of the harbor.

(c) The bluffs, currently under erosive wave attack between 5,000 and 7,000 feet south of the harbor, are very high so that erosion rates measured in feet per year are low but the corresponding volume rates (in cubic yards per foot) are high.

The shorelines apparently have become comparatively stabilized since about 1933.

## 2. Geomorphology.

Figure 13 shows the nearshore bathymetry determined by a survey in April 1973. Beach profiles from this survey and one in May 1945 are summarized in Figure 14. Three or four lines of longshore bars are prominent most of the time and occur in water depths to approximately 30 feet. The first bar, in depths of 1 to 4 feet, can change rapidly from storm to storm and is often broken into short segments from 200 to 1,000 feet long by rip channels. Adjacent to the breakwaters, the rip channels tend to elongate lakeward as far as the second bar. The second and third bars, occurring in depths of 6 to 14 feet, appear to be affected only by larger storm waves and are relatively continuous along the shore. Aerial photos show that these bars tend to lose their prominence as they approach the breakwaters from both sides, suggesting that prevailing erosion exists across the bar crests near the breakwaters. The fourth bar occurs at depths of 15 to 20 feet about 1,500 feet offshore and is characterized by crescentic crests displaying wavelengths between 3,000 and 5,000 feet. A crescentic fourth bar with an average wavelength of about 5,000 feet existed north of Holland Harbor, but none existed on the south side.

Although the general bathymetry follows the coastline, significant departure from this trend occurs in a region offshore of the Holland Harbor breakwaters (Fig. 15). The 24-, 27-, and 29-foot-depth contours meander sharply off the

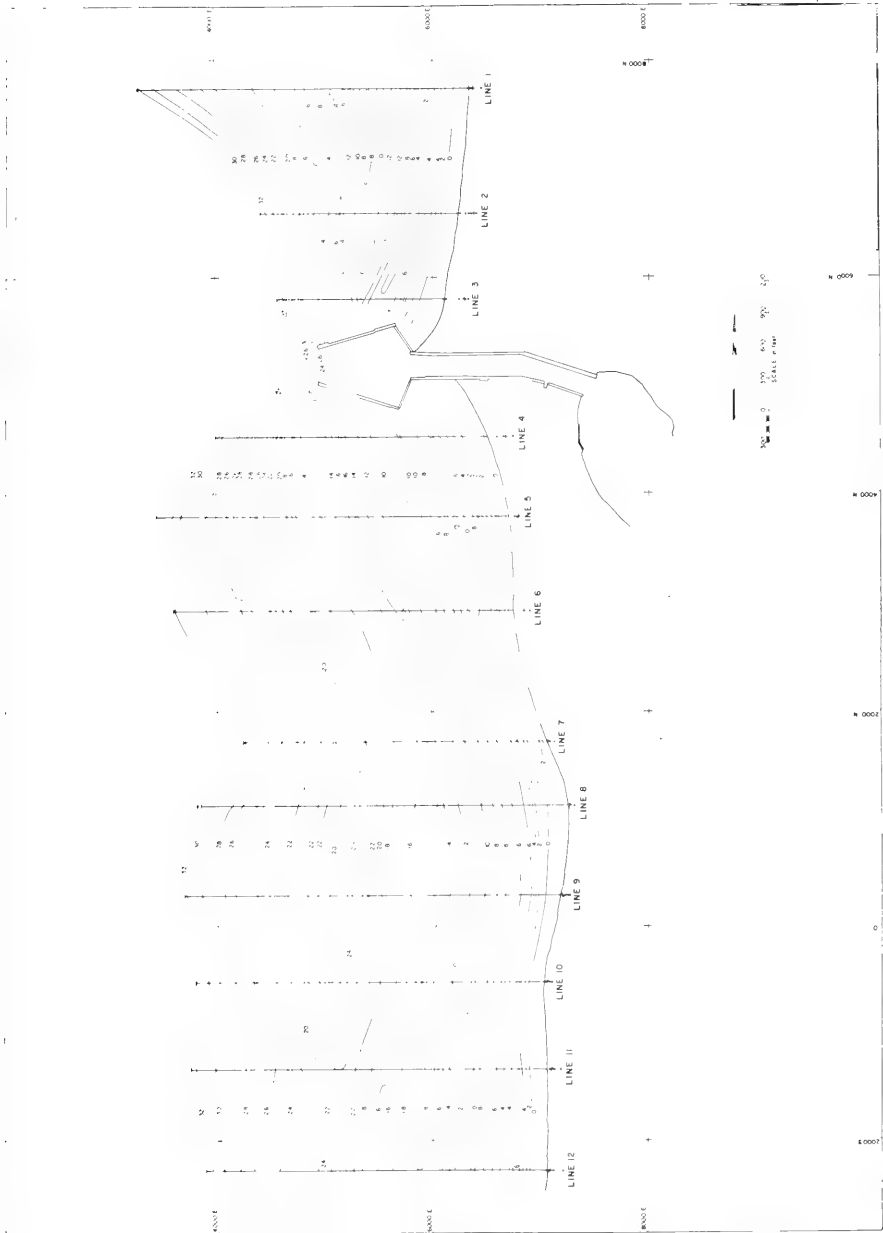


Figure 13. Nearshore bathymetry, Holland Harbor (from U.S. Army Engineer District, Detroit, 1975).

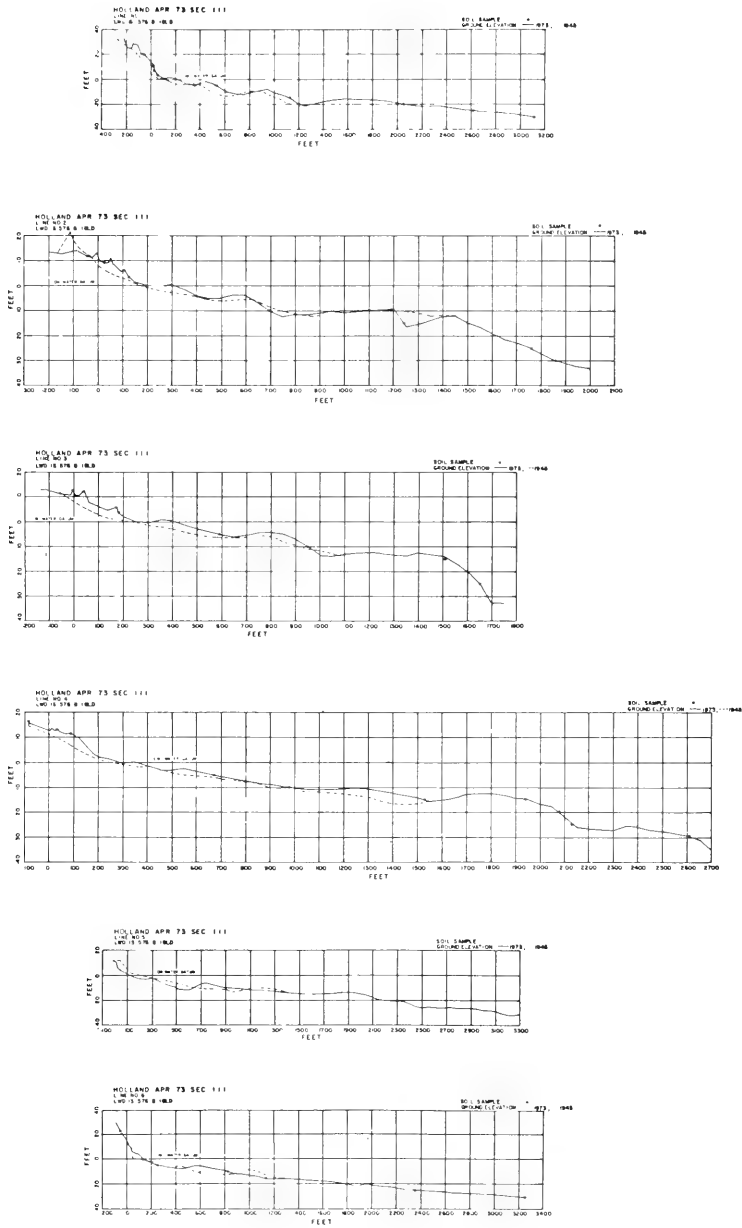


Figure 14. Beach profile summaries for Holland Harbor (from U.S. Army Engineer District, Detroit, 1975).

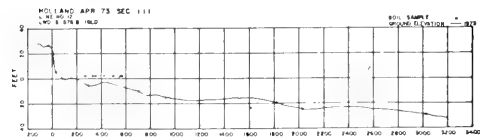
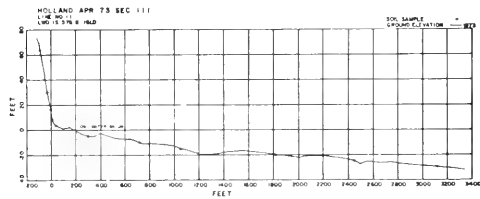
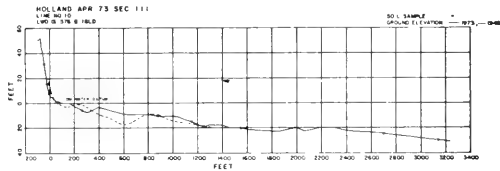
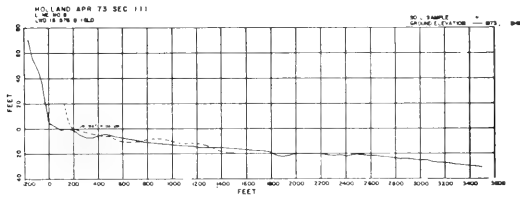
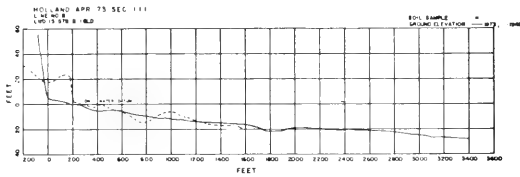
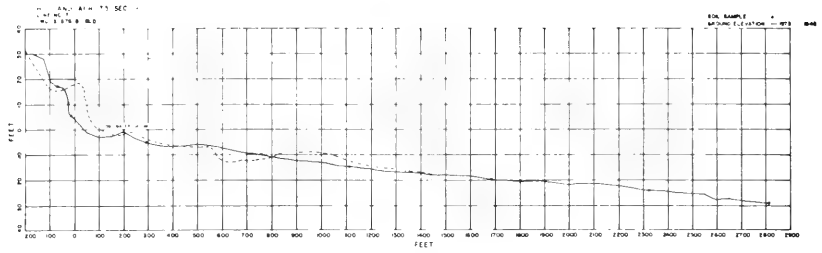


Figure 14. Beach profile summaries for Holland Harbor (from U.S. Army Engineer District, Detroit, 1975).--Continued

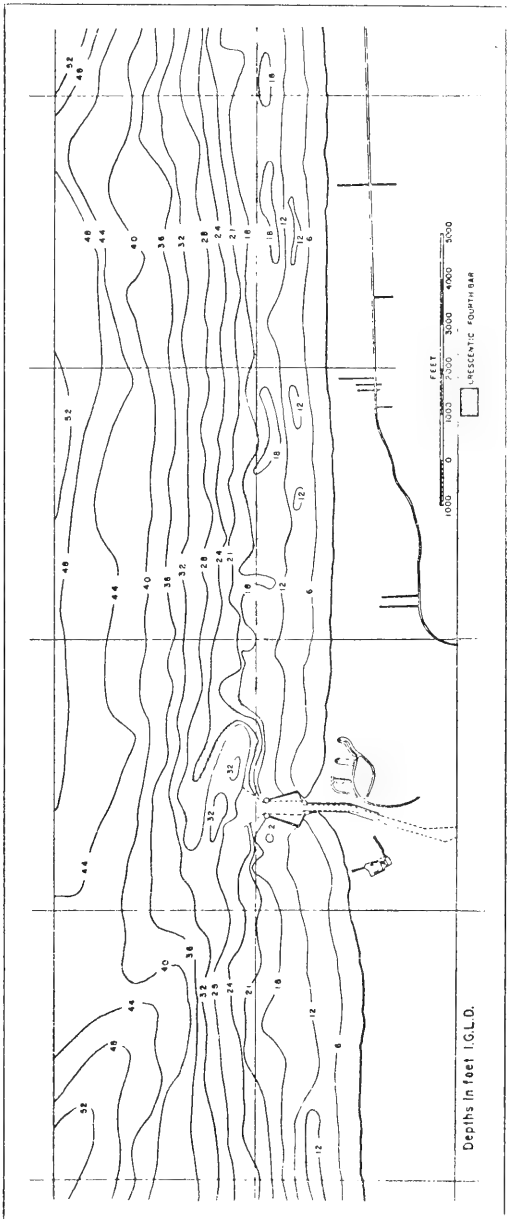


Figure 15. Holland Harbor nearshore bathymetry (from U.S. Army Engineer District, Detroit, 1975).

harbor entrance, delineating a ridgelike formation which extends obliquely lakeward from north to south. Deeper contours to the southwest of this formation suggest that it may extend as deep as 50 feet. The ridge has a maximum height of approximately 7 feet, and occurs due west of the harbor entrance. Between the ridge and the harbor entrance is a steep trough about 34 feet deep. A lack of survey data before the harbor construction prevents a reliable conclusion as to whether or not this underwater ridge was caused by the presence of the breakwaters. However, the possibility cannot be ruled out that it was formed by the littoral drift arriving predominantly from the north and flushed lakeward by the breakwater. This material, unable to return shoreward due to the absence of significant swell activity in this region, could have accumulated to form such a formation on the offshore bed over a long period. Implications of this interpretation are significant because it may mean that little, if any, bypassing material across the harbor entrance could be expected to reach the southern shore of Holland Harbor.

Many of the dunes reach a height of 150 feet, and in a few places exceed 200 feet above the lake level. The highest dunes are confined to a belt about 1 mile wide but lower ones occur for a width of several miles near Holland. Dune building by wind action is still active. North of Holland Harbor some low dunes are actively migrating inland or leeward from the bluff onto relatively level upland. In this area the dunes are 40 to 120 feet high. At numerous places, slumping of vegetation is evident on the bluff slopes. South of Holland the dunes are higher, frequently more than 200 feet above lake level. The dunes are well vegetated except for occasional blowouts on larger dunes.

At many places, dunes descend directly to the lake or to a narrow strip of beach up to approximately 50 feet in width. The only area near Holland Harbor where a substantial beach exists is about 2,000 feet immediately north and about 500 feet immediately south of the breakwaters. Maximum beach width in this area is about 500 feet on the north side and 150 feet on the south side, indicating the predominance of littoral drift from the north. Berm development is generally poor for many miles of shoreline north of Holland. Berms develop more frequently south of Holland, growing to an average height of 1 foot in the swash zone. These berms are usually truncated at positions of a recessed shoreline where a rip current has gouged a deep channel across the surf zone.

### 3. Littoral Materials.

The dominant littoral material which comprises dunes, beaches, and nearshore lake bottom is glacial sediment belonging to a fine sand category (less than 0.42 millimeter in median diameter). Scattered pebbles are found both on the dunes and the lake bottom. Sand-sized material is dominantly quartz (80 to 85 percent) with up to 12 to 15 percent feldspar. Heavy materials represent only 2 to 3 percent.

a. North of Holland Harbor. An analysis of bluff, foreshore (above low water datum) and bottom samples indicates that the majority of these sands belong to the fine sand category. (The Unified Soil Classification System defines fine sand as ranging in size from 0.42 to 0.074 millimeter (1.25 to 3.75 phi), and medium sand as ranging from 0.42 to 2.0 millimeters or 1.25 to -1.00 phi). North of the harbor, the average bluff and foreshore sand consists of 88.0 percent fine sand and 11.7 percent medium sand; the average lake bottom sand consists of 95.0 percent fine sand and 5.0 percent medium sand. A general



trend exists for the sand size to become progressively smaller from foreshore to offshore. Average median diameters are 0.34 millimeter at the foreshore, 0.28 millimeter at depths of 5 and 10 feet, 0.23 millimeter at depths of 15 and 20 feet, and 0.18 millimeter at depths of 25 and 30 feet. Dune and bluff sand is somewhat finer than the foreshore sand, but coarser than the lake bottom sand. There is little systematic variation in sand size with distances from the breakwater. Sorting ranges between 0.28 and 0.40 phi, indicating very good sorting; sorting varies little between dune, foreshore, and the 5-foot depth and becomes poorer toward deeper water, reaching approximately 0.40 phi at depths of 20 and 30 feet.

b. South of Holland Harbor. The majority of the sands from the dune, the bluff, the foreshore, and the lake bottom on the south side of Holland belong to the fine sand category. Generally, only minor differences exist between average sands from the north and the south sides of Holland. The average bluff and foreshore sand consists of 85.1 percent fine sand (finer than 0.42 millimeter) and 14.9 percent medium sand. The average lake bottom sand consists of 94.7 percent fine sand and 5.3 percent medium sand. Median diameters decrease from foreshore toward offshore, about 0.25 millimeter at depths of 5 and 10 feet, about 0.20 millimeter at depths of 15 and 20 feet, and about 0.16 millimeter at depths of 25 and 30 feet. Dune and bluff sand is finer than the foreshore sand but coarser than the lake bottom sand. The lake bottom sands are distinctly coarser immediately south of the harbor and also along lines 11 and 12 (Fig. 13), about 6,000 feet south of the harbor. Sorting displays a wider scatter than on the north side of Holland, ranging between 0.3 and 0.5 phi. As on the north side, sorting becomes poorer from foreshore toward offshore.

The principal sources of littoral material are the beach and the bluff. Generally along eastern Lake Michigan, and particularly near Holland Harbor, the supply of littoral material from major inland water runoff is negligible. For this reason, the long-term geologic trend appears to be for sediment from shore erosion to fill in the lake.

c. Shoaling and Dredging. Shoaling and dredging records indicate that the annual shoaling in the entrance channel of Holland Harbor averaged about 25,000 cubic yards for the period 1965-70. The pattern of accretion shows some yearly variation and indicates that material encroaches into the entrance area from both north and south. In addition, the relative amount of drift from north and south appears to vary from year to year. Figure 16 shows conditions at the harbor entrance before dredging in 1973 and 1974.

#### 4. Meteorology.

The dominant factors are winds, waves, and water level variations. The winds and waves are directly responsible for sediment movements, and fluctuations of water levels separate the regimes of the two areas affected, i.e., the backshore above the waterline and the foreshore below the waterline.

a. Winds. Winds are a dominant force affecting the Holland Harbor area; they produce a number of major effects by (a) generating a force for waves, (b) causing lake level changes, and (c) transporting sand across the beaches, particularly the finer sediment sizes. Wind data (available from ship reports) over the southern half of Lake Michigan (south of 44° N.) show that more than

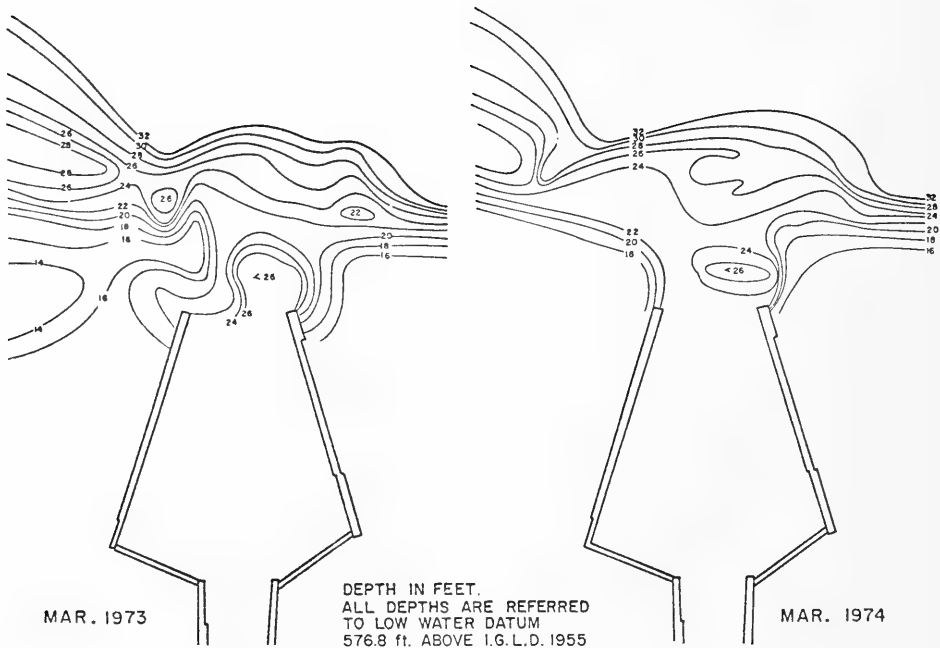


Figure 16. Conditions at Holland Harbor entrance before dredging in 1973 and 1974 (from U.S. Army Engineer District, Detroit, 1975).

21,000 observations were taken from 1963 to 1973. These data have been summarized for a 12-month period (Fig. 17,A) and for a 9-month ice-free period (Fig. 17,B). A 3-month ice period would correspond to a severe winter.

b. Waves. Sources of wave data for Lake Michigan were (a) Summary of Synoptic Meteorological Observations (SSMO) (National Oceanic and Atmospheric Administration (NOAA), 1963-73); (b) Saville (1953); (c) Cole and Hilfiker (1970); and (d) Littoral Environment Observation (LEO) program data from the U.S. Army Coastal Engineering Research Center (CERC).

Figure 18 shows deepwater wave roses for an average 12-month period and for an assumed 9-month ice-free period, respectively, in southern Lake Michigan. Comparison of these wave and wind roses reveals a close agreement with the wind and wave statistics. Dividing wave heights into two groups (i.e., by heights lower and higher than 4.1 feet), the low waves occur most frequently from the south, while the high waves occur predominantly from the north.

Figure 19 shows exceedance probabilities of deepwater waves based on SSMO and hindcast data of Saville (1953) and Cole and Hilfiker (1970). Only those waves which occur during a 9-month ice-free period and are traveling shoreward are included in the statistics. The three statistics generally agree quite well for wave heights up to about 8 feet. For wave heights larger than 8 feet (which occur only about 1 percent of the time), a discrepancy between the three is evident. The SSMO data show a less frequent occurrence of higher waves, but

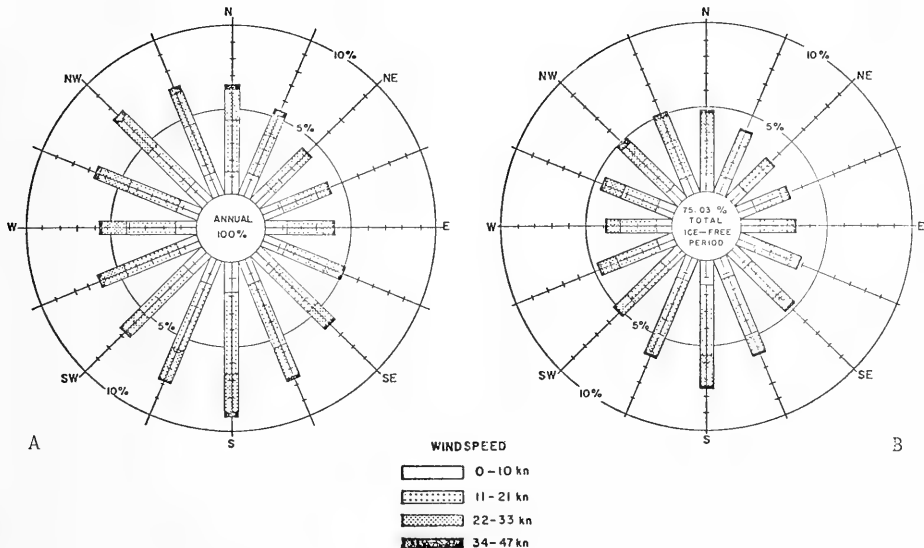


Figure 17. Wind rose for an average 12-month period (A) and for an average 9-month ice-free period (B) for southern Lake Michigan (data from SSMO observations, 1963-73).

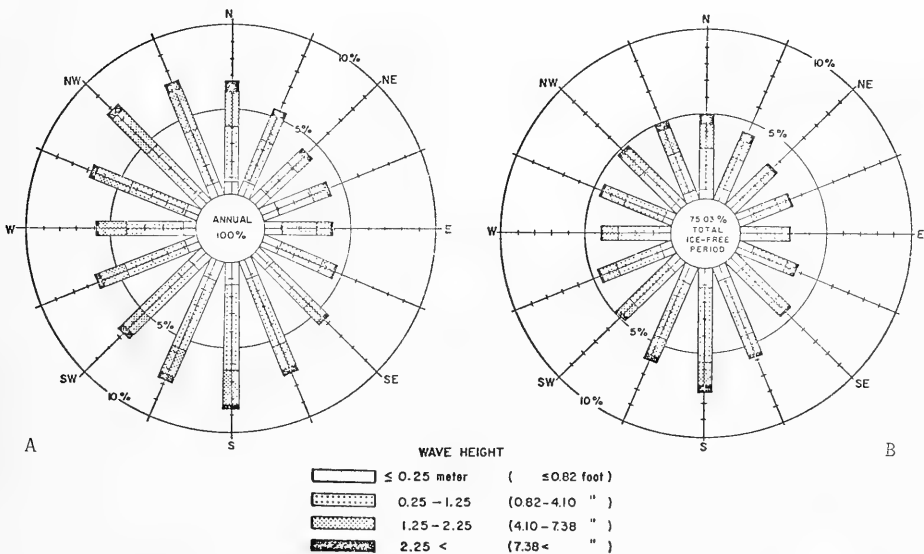


Figure 18. Wave rose for an average 12-month period (A) and for an assumed 9-month ice-free period (B) for southern Lake Michigan (data from SSMO observations, 1963-73).

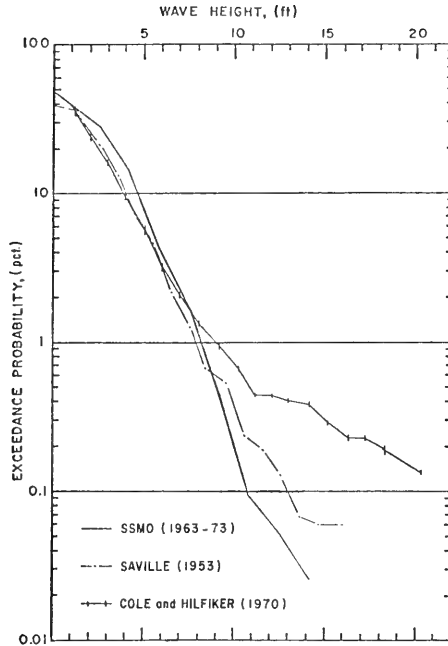


Figure 19. Wave height exceedance probabilities (9-month ice-free period).

this may be partly due to the fact that ships tend to avoid storms. This may also be less true for the higher windspeeds; hence, the frequency of occurrence of high waves may tend to be overestimated. The disagreement between Saville's and Cole and Hilfiker's hindcast data probably results because Saville's data are based on coastal winds which are generally weaker than those on the deep-water lake surface. Figure 20 summarizes the probability of occurrence of various wave heights as a function of the month of the year.

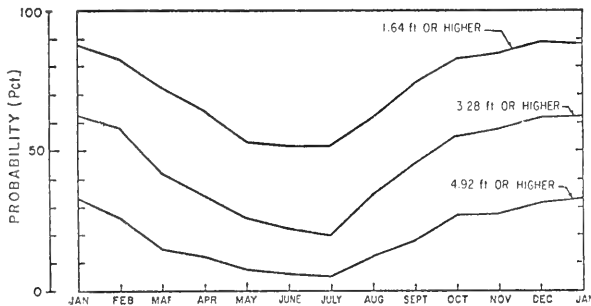


Figure 20. Variations of probability of various wave heights with months of the year.

## 5. Hydrology.

a. Water Level Variations. Figure 21 summarizes the observed mean monthly lake levels since 1920. Records are available back to 1860.

b. Currents. Currents in the Holland area are variable. They generally appear to take a northward set during the summer and a southward set during the winter in response to the prevailing winds although reversals are frequent. There also appears to be evidence of a rotational current system in Lake Michigan which is not very well understood. In the immediate nearshore area it is likely that the currents are wave induced and will propagate alongshore in the direction of the dominant waves at the time. Inshore of the first bar, rip currents are extremely well developed and can add a significant amount of offshore water movement to the general longshore current. Intensity of the rip currents is evident from a number of rip channels which are gouged 1 to 2 feet below the adjacent ground. Longshore currents approaching Holland Harbor are deflected lakeward along its breakwaters. Aerial photos indicate that the deflected current, after bypassing the harbor entrance, will move a considerable distance lakeward before turning parallel to and toward the shore off the down-drift coast.

c. Ice. Floating ice is common in the Holland Harbor area during the winter months. Ice accumulates on the beach by wind and wave action and reportedly often extends in a solid mass from the shoreline to more than 1,000 feet offshore. Wave heights are substantially decreased within an ice field and ice along the shore blocks wave action to some extent. However, the action of ice can accelerate erosion processes; e.g., ice being pushed upon the beach will loosen consolidated beach and bluff material and some of the sediment becomes embedded in the ice at the shore and over the longshore bars to be carried elsewhere if the ice drifts away during the spring thaw. The average ice season at Holland Harbor extends from late December to late March.

## 6. Littoral Drift Estimate from Wave Statistics.

Littoral drift has been computed from the available wave statistics discussed earlier. The governing relationship used was (U.S. Army, Corps of Engineers, Coastal Engineering Research Center, 1977)

$$Q = 0.000133 E_{\alpha}$$

where  $Q$  is the potential littoral drift in cubic yards per day, and  $E$  the longshore momentum flux in feet per pound per day per foot of beach. The relationship between  $\alpha_D$  and  $\alpha_O$  is determined from linear theory in assuming that the bottom contours are straight and parallel. The number of waves per day for each wave height period-direction class is given by

$$n = \frac{864 \times 10^2}{T} p$$

where  $p$  is the probability of occurrence of that wave class. Computations were made using the wave statistics from SSMO data, Saville (1953), and Cole and Hilfiker (1970). The duration of computation is for the 9-month ice-free period from late March to late December.

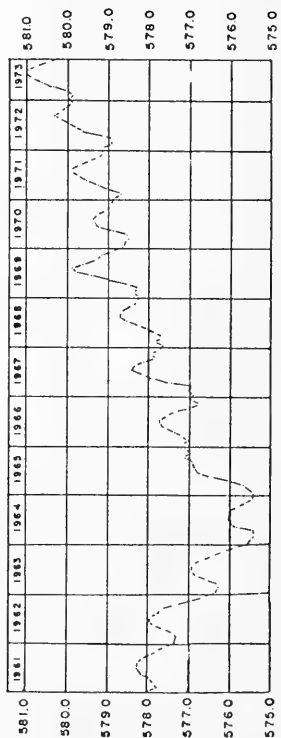
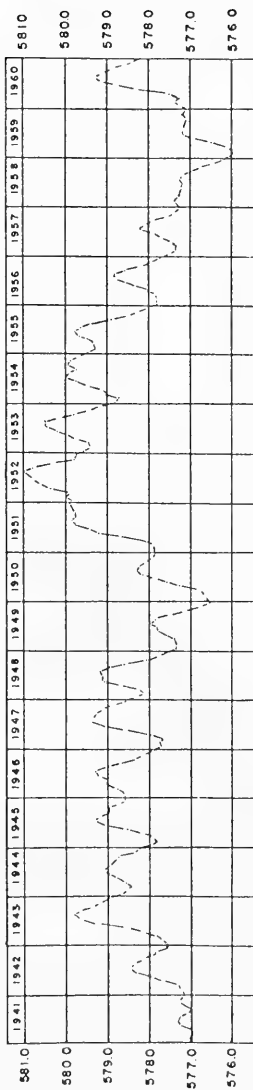
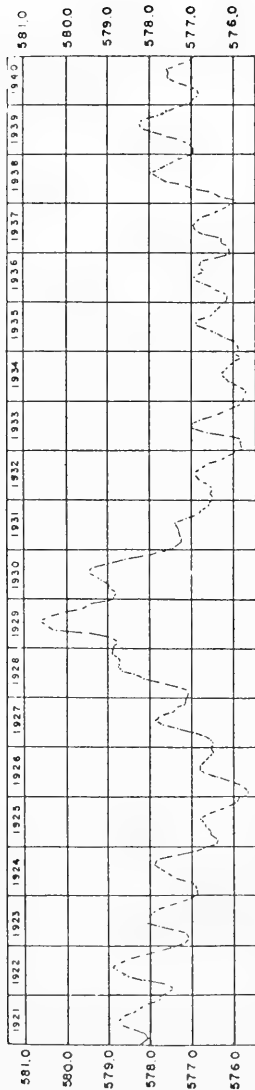


Figure 21. Mean monthly lake levels since 1920 (from U.S. Army Engineer District, Detroit, 1975).

All of the littoral drift computations show a large gross drift of 300,000 to 500,000 cubic yards, defined as the sum of all north and south movement, regardless of direction, whereas the net drift is much smaller. Individual yearly predictions show a wide variability in net littoral drift quantities.

The littoral drift is predicted to be from south to north with a mean value of more than 265,000 cubic yards. The SSMO data and Coles and Hilfiker's wave statistics lead to the prediction of 61,000 and 76,000 cubic yards, respectively, from north to south. This direction is consistent with the observed growth of the fillets on each side of the harbor, the north side showing a much greater accretion.

Figure 22 summarizes the monthly fluctuations of littoral drift based on the SSMO data. The figure shows that the monthly drift is large during late fall when the activity of extratropical cyclones intensifies in these regions, and small during the summer months, especially in June, when wave heights are generally smaller.

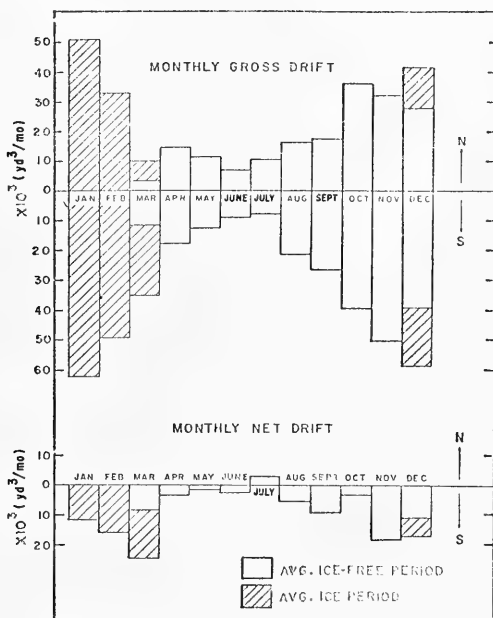


Figure 22. Monthly variations of computed gross and net littoral drifts for Holland, Michigan.

## 7. Analysis of Aerial Photos.

A sequence of eight sets of aerial photos of Holland Harbor taken over the interval 27 July 1950 to 5 October 1973 was analyzed to assess the long-term evolutionary development of the shoreline. A regression analysis was performed to correct the shoreline for lake level variations and to determine the long-term erosion-accretion rates along the coast.

Table 1 presents shoreline positions (with and without lake level corrections) as a function of distance along the coast, as determined from the aerial photos. The corrected shoreline positions are referenced to a common lake level of 578.5 feet, as determined by a regression against lake level. Figure 23 shows the 1973 Holland Harbor shoreline. The origin of the coastline coordinate is taken at the harbor, positive in the north direction. The shoreline position was measured at 290-foot increments along the coast.

A regression of shoreline position against lake level and time provided an estimate of the long-term evolutionary trend of the shoreline at each station along the coast. The regression study revealed general erosion extending south of the harbor and accretion immediately north of the harbor. Over an 8,410-foot span south of the harbor, the average beach erosion rate was 0.75 foot per year. Over a 4,060-foot span immediately north of the harbor, the average accretion rate was 1.65 feet per year. A span of 10,585 feet, starting 4,930 feet north of the harbor, had an average erosion rate of 1.28 feet per year. These evolutionary trends of the shoreline include natural effects as well as any effects which can be attributed to the harbor.

Figure 24 shows the evolutionary smoothed trend (defined as the average accretion or erosion rate between 1950 and 1973) along the coast near Holland Harbor. Erosion dominates south of the harbor, accretion immediately north, and erosion again farther north of the harbor. The smoothed curve in Figure 20 demonstrates that the accretion resulting from the harbor extends about 5,000 feet north of the harbor. These estimates of the evolutionary trend of the shoreline are subject to large annual and spatial fluctuations.

#### 8. Comparisons of Profiles from 1945 and 1975 Surveys.

The surveys of May 1945 and April 1973 (lake levels at 578.4 and at 580.1 feet, International Great Lakes Datum (IGLD), respectively) permit a comparison of profile changes from which sediment volume changes can be estimated. Since the actual profile locations in the two surveys did not coincide (in general), the 1945 survey was interpolated on the lines of the 1973 survey to allow a comparison. Table 2 summarizes the cross-sectional area changes and the volume computations in two parts (above and below low water datum). The last column in the table gives the erosion or accretion rates determined from the aerial photos.

The average volumetric accretion rate on the north side (from ground survey data) is 2.13 cubic yards per year per foot of shoreline for 1,950 feet (450 to 2,400 feet north of the breakwater) compared with the average shoreline accretion rate of 1.92 feet per year for this same region determined from Figure 20. The average volumetric erosion rate on the south side of the harbor from the survey comparisons is 1.41 cubic yards per year per foot of beach, whereas the values from Figure 20 for the south stretch (470 to 5,550 feet south) give 0.82 foot per year as an average rate of shoreline erosion. The agreement on the north side indicates that the approximation of 1 square foot of beach per cubic yard is reasonably valid, whereas on the south side this is less true. The discrepancy on the south side is related to the bluff erosion contribution. The main erosion rate below the low water datum level is only 0.16 cubic yard per year per foot. Hence, the bluffs contribute at least an additional 1.25 cubic yards per year per foot, which exceeds the conditions for the approximation of 1 square foot of beach to correspond to 1 cubic yard of material.





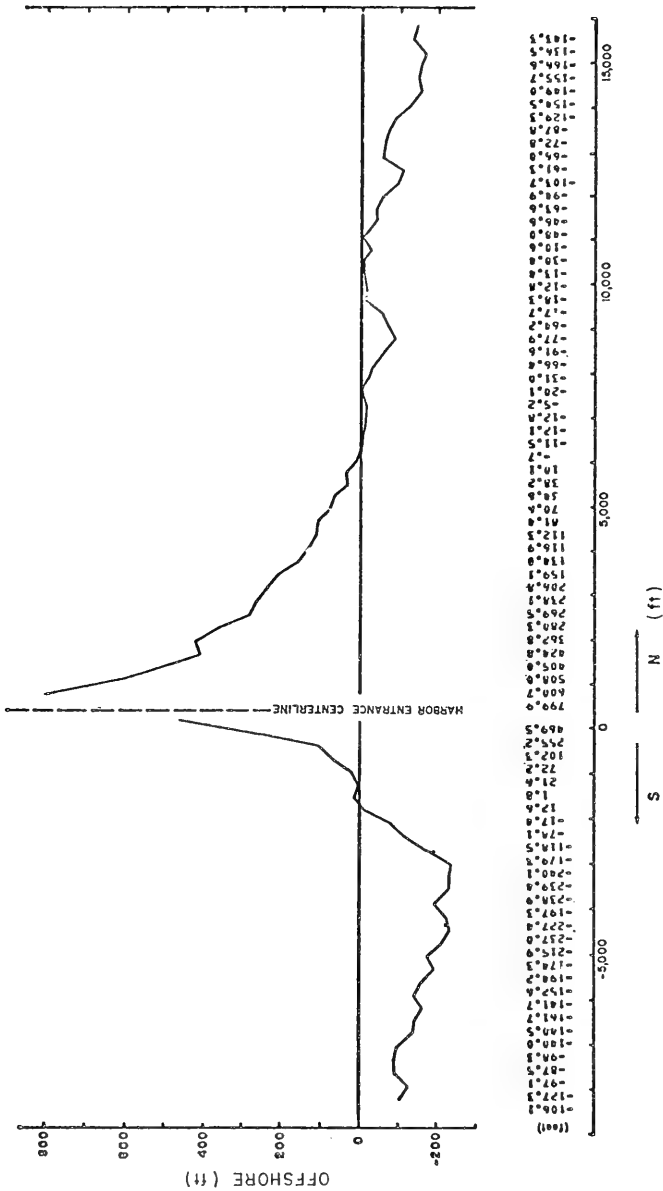


Figure 23. Shoreline positions at Holland, Michigan, in 1973, as determined by aerial photos.

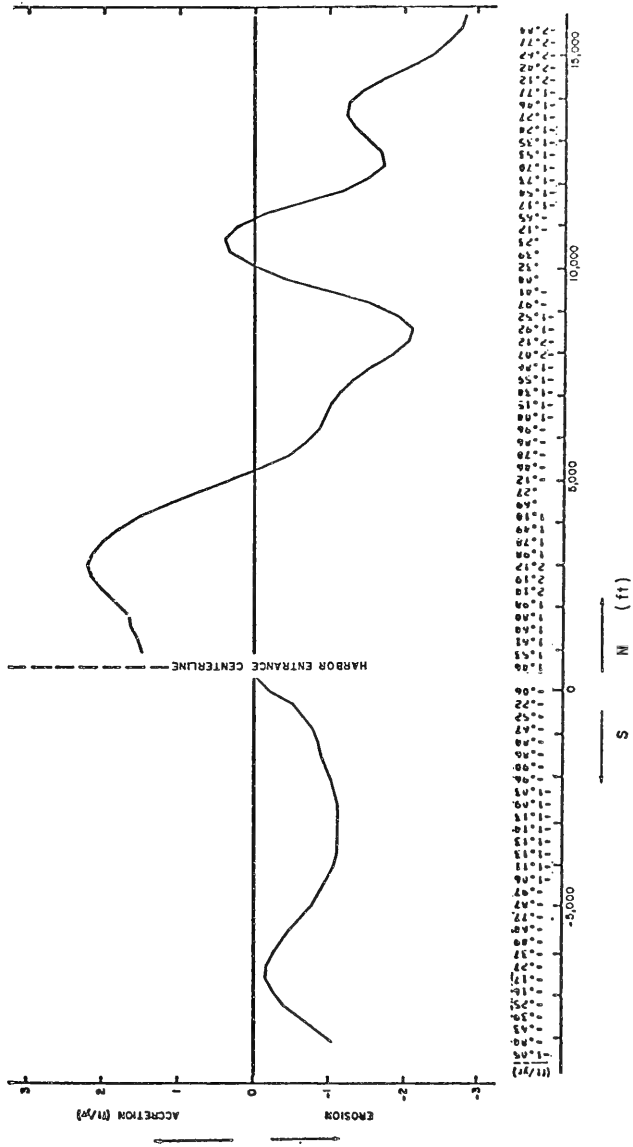


Figure 24. Smoothed average rates of shoreline erosion and accretion (feet per year) at Holland, Michigan.

Table 2. Summary of cross-sectional changes and computed volumetric changes for 1945 and 1973 surveys.<sup>1</sup>

Line No.	Distance between profiles (ft)	Above LWD		Below LWD		Total mean vol. change rate (1945-73) (yd <sup>3</sup> /yr/ft)	Mean observed shoreline accretion-erosion change rate (1950-73) (ft/yr)
		Cross section area change (ft <sup>2</sup> )	Avg. rate of vol. change (yd <sup>3</sup> /yr/ft)	Cross section area change (ft <sup>2</sup> )	Avg. rate of vol. change (yd <sup>3</sup> /yr/ft)		
1	1,150	2,298	+1.47	1,528	+1.10	+2.57	+2.0
2	800	-78	+0.84	134	+0.65	+1.49	+1.8
3		1,347		855			
Harbor							
4	740	2,144	+1.16	928	+0.30	+1.46	-0.3
5	880	391	+0.17	-479	-0.53	-0.36	-0.6
6		642		-324	-0.72	-0.96	-0.9
7	1,210	821	-0.24	-761	-2.80	-3.71	-1.0
8	605	-562	-0.91	-3,480	-3.39	-4.98	-1.2
9	830	-1,848	-1.59	-1,660	-0.88	-0.49	-0.9
10	815	+2,431	+0.39	305			

<sup>1</sup>+ = accretion; - = erosion

As demonstrated previously in the analysis of the aerial surveys, the harbor influence on the north side extends about 4,200 feet. Farther north it is assumed that the observed erosion rate will be close to the natural erosion rate for this area of the Lake Michigan coast. At 4,200 to 15,400 feet to the north of Holland Harbor, the average erosion rate during the 1950-73 period (from aerial photos) was 1.28 feet per year per foot of shoreline. If the approximation of 1 cubic yard of volume per square foot of beach is used, the corresponding sediment volume loss is 1.28 cubic yards per year per foot of shoreline plus the erosion rate of the dunes. The bluffs which have an average height of about 40 feet in this area would contribute an additional sediment loss of  $40 \times 1.28/27 = 1.90$  cubic yards per year per foot. Hence, the total sediment loss to the offshore in this area is estimated to be averaging  $1.90 + 1.28 = 3.18$  cubic yards per year per foot of shoreline during the past 23 years. This rate of loss is considered to represent the natural rate of loss for littoral sediments in the Holland area due to all factors except the navigation structure. It must be remembered that the erosion rate of 3.18 cubic yards per year per foot of shoreline is an average rate for the past 23 years (1950-73). Since lake levels have been much higher during the past few years, the present erosion rate must be expected to be higher than the average and therefore will probably exceed 3.18 cubic yards per year per foot of beach.

## 9. Sediment Budget.

a. North Side. An independent evaluation of the net littoral drift has been obtained from various surveys as summarized below in which a sand budget analysis is made for the north side of Holland Harbor. The shoreline changes shown in Figure 25 provide information for an area measurement of accretion. An approximation for volumetric accretion can subsequently be made from the relationship, wherein 1 square foot of change in beach surface area equals 1 cubic yard of beach material. This relationship has previously been shown to be reasonably valid for the north side. Subsequent corrections may be necessary because of the dune-building phenomenon.

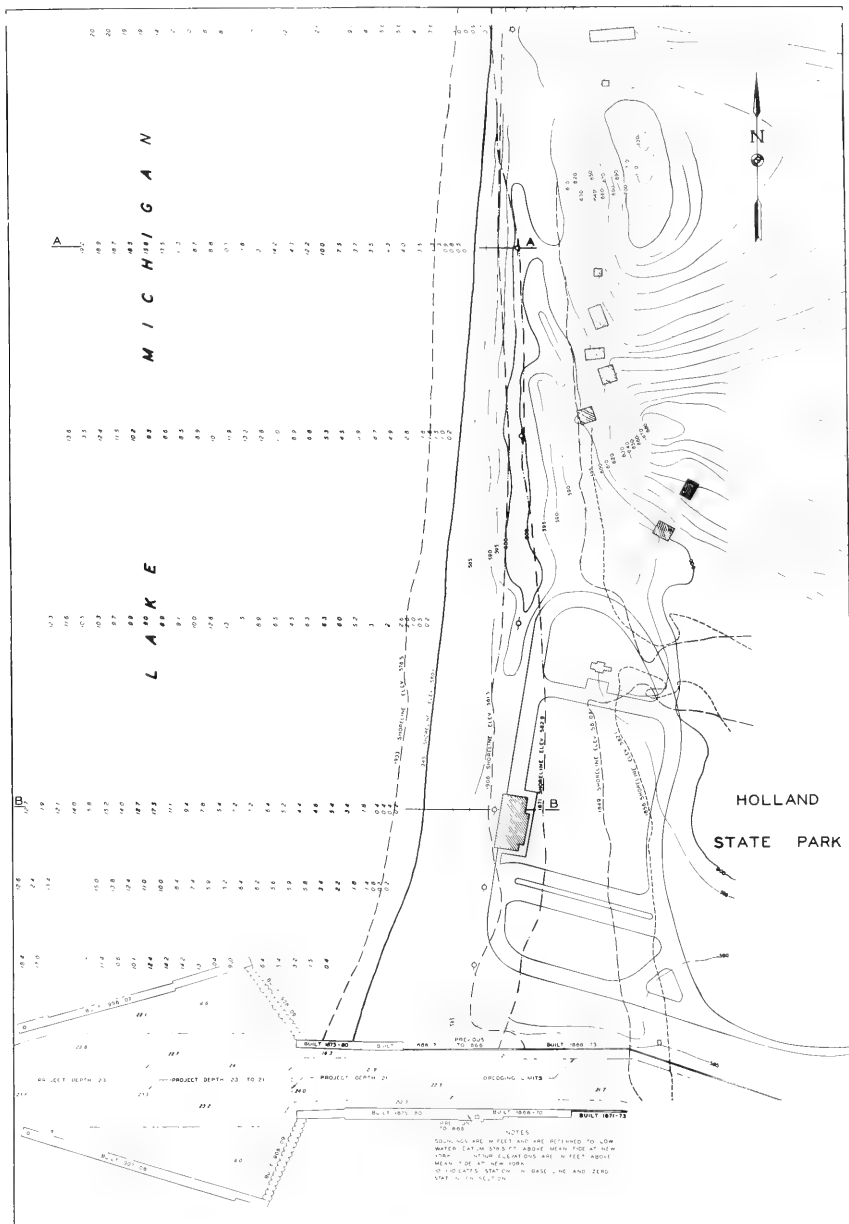


Figure 25. Historical shorelines north of Holland, Michigan, between 1849 and 1945 (from U.S. Army Engineer District, Detroit, 1975).

The area changes corresponding to the waterline shown in Figure 21 were determined for a length of shoreline extending 2,550 feet north of the north breakwater. These areas are summarized in Table 3. A correction is applied for the variation in lake level by the relationship

$$\text{Correction in 1,000 square feet} = \frac{45 \times \text{lake level difference} \times 2,550}{1,000}$$

which follows the assumption of an average beach slope of 1 on 45 for this area as determined from the 1945 surveys.

Table 3. Summary of shoreline accretion rates north of Holland Harbor (1849-1945).

Year	Measured area from breakwater to 2,550 feet north (1,000 ft <sup>2</sup> )	Lake level (N.Y. datum) (ft)	Lake level difference (ft)	Area correction (1,000 ft <sup>2</sup> )	Net area (1,000 ft <sup>2</sup> )	Rate (1,000 ft <sup>2</sup> /yr)
1849	714	581.0	----	----	714	-13.3
1856	495	582.1	+1.1	+126	621	+51.9
1871	1,181	582.9	+1.9	+218	1,399	+3.4
1906	1,462	581.5	+0.5	+57	1,519	+13.7
1933	2,175	578.5	-2.5	-287	1,888	+13.4
1945	1,941	580.1	+0.9	+108	2,049	

The results of the computations (Table 3) indicate rates of accretion varying from 3,400 to 51,900 cubic yards per year if the general rule of 1 square foot of beach area corresponds to 1 cubic yard of beach material is applied. These accretion rates should be interpreted according to the history of the construction. The first breakwaters were constructed in 1856-60 and trapped most, if not all, of the littoral drift. Since the accretion of 51,900 square feet per year during the period 1856-71 is an average, then the corresponding littoral drift rate must have exceeded 51,900 cubic yards per year (it must be assumed that by 1871 some of the littoral transport was passing around the breakwater heads into the navigation channel).

The accretion was slowed to 3,400 square feet per year from 1871 until the harbor breakwater extensions were started in 1906. Therefore, the littoral transport passing around the north breakwater must have been quite high from 1871 to 1906; also, the building of new dunes by wind action probably occurred during this period.

From 1906 to 1933 the accretion averaged 13,700 square feet per year; after 1933 this rate dropped slightly to 13,400 square feet per year. However, some inland dune building could still be taking place. Measurements from the 1945 survey show an accumulated volume of 137,400 cubic yards above elevation 585 (1945 datum) on the north side of Holland Harbor. This volume would only account for about 1,900 cubic yards per year from 1871 to 1945 but windblown sand losses farther inland would increase this.

The detailed analysis of aerial photos taken from 1950 to 1973 indicates an average accretion rate of about 1.65 feet per year per foot of shoreline for the first 4,000 feet of shoreline north of the harbor, a total of 6,600 square feet per year. The accretion rate based on a comparison of the 1945 and 1973 hydrographic surveys for profiles 1, 2, and 3 in Figure 10 was about 4,800

cubic yards per year for the first 2,550 feet north of the breakwater. The incoming littoral drift supply must be providing the observed accretion since there are expected offshore losses of 3.18 cubic yards per year per foot of shoreline for the first 4,000 feet of shoreline north of the harbor, and material is apparently being accumulated in the dunes in Holland State Park.

To summarize the present situation, it is believed that about 61,000 cubic yards of littoral material is being transported toward Holland Harbor from the north. The disposition of this material is summarized in Figure 26. About 12,700 cubic yards per year is lost offshore ( $3.18 \times 4,000$ ), 6,600 cubic yards per year is accumulating on the beach face on the north side, and about 1,900 cubic yards per year is being accumulated in the dunes of Holland State Park. Although the exact amount is unknown, an estimated 1,300 cubic yards per year of sand is lost inland. Hence, it is calculated that about 38,500 cubic yards per year of sand arrives at the harbor entrance but at the most 25,000 cubic yards is trapped. It is likely that some of the 25,000 cubic yards dredged in the harbor entrance comes from the south side; therefore, at least 13,500 cubic yards per year is lost offshore. Consequently, it is concluded that the harbor structures cause a loss of materials from the littoral region of at least 13,500 cubic yards per year. In addition, the 25,000 cubic yards per year that is dredged is dumped offshore. The overall result is that the south side of the harbor is being starved of 61,000 cubic yards per year.

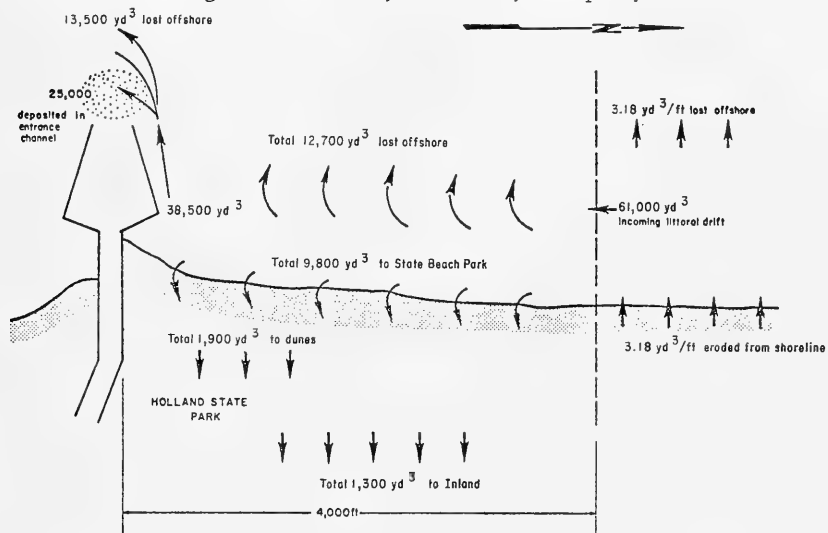


Figure 26. Summary of sand budget north of Holland, Michigan.

b. South Side. Figures 27 and 28 provide information for an area measurement of shoreline accretion and erosion. The beach area changes are summarized in Table 4 by areas north and south of a section located 1,200 feet south of the south breakwater (an arbitrarily selected station which appears to correspond to a stationary shoreline point for the period 1856-1945). The table summarizes the corrections in lake level variation about an average offshore beach slope of 1 on 24.5 for the first 1,200 feet south, and an average beach slope of 1

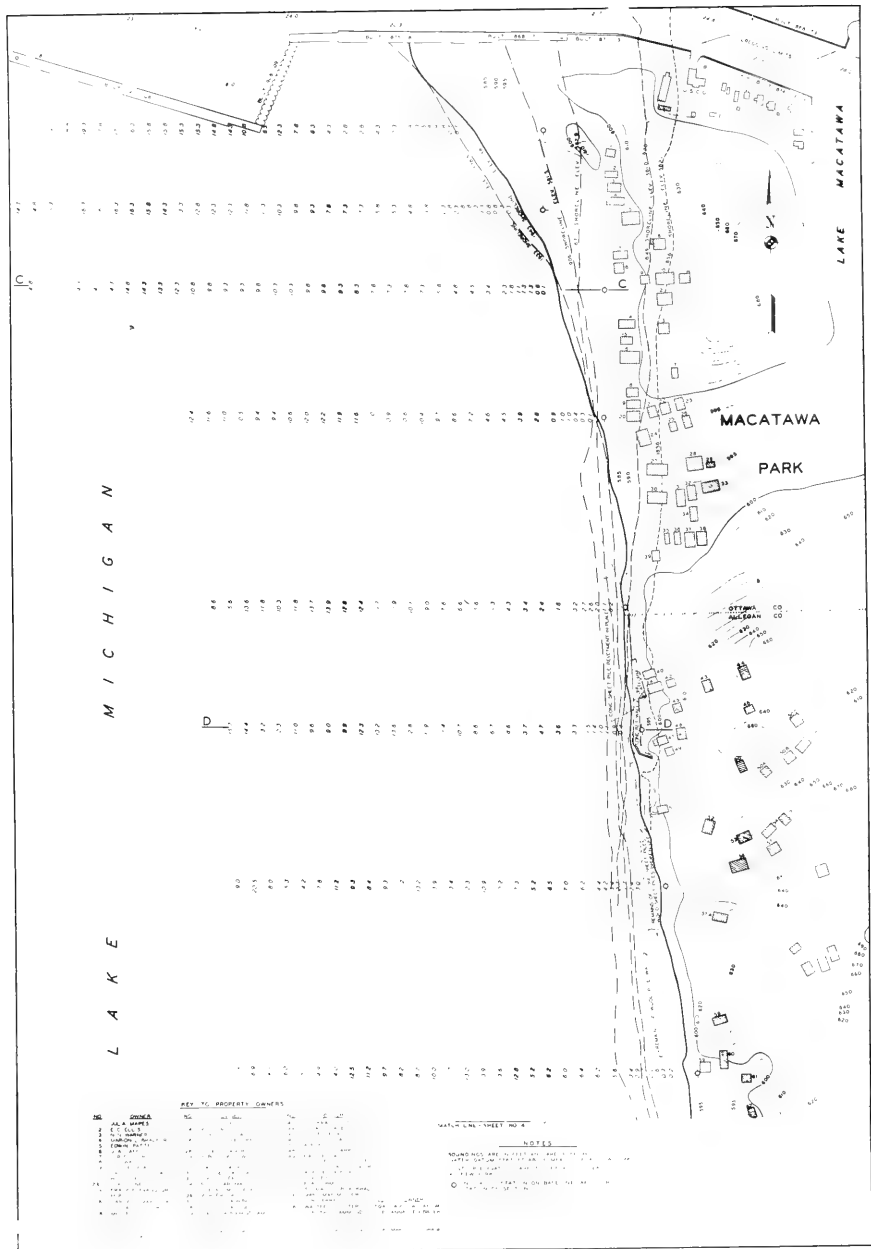


Figure 27. Historical shorelines immediately south of Holland, Michigan, between 1849 and 1945 (from U.S. Army Engineer District, Detroit, 1975).





Table 4. Summary of beach area changes south of Holland Harbor.

Year	Measured area (1,000 ft <sup>2</sup> )	Lake level (N.Y. datum) (ft)	Lake level difference (ft)	Area correction (1,000 ft <sup>2</sup> )	Net area (1,000 ft <sup>2</sup> )	Rate (1,000 ft <sup>2</sup> /yr)
Breakwater to 1,200 feet south						
1849	184	581.0	---	---	184	
1856	104	582.1	+1.1	+22	126	-8.3
1871	433	582.9	+1.9	+37	470	22.9
1906	497	581.5	+0.5	+10	507	1.1
1933	688	578.5	-2.5	-49	639	4.9
1945	647	580.1	+0.1	+2	649	0.8
1,200 to 3,600 feet south of breakwater						
1849	530	581.0	---	---	530	
1856	391	582.1	+1.1	+37	428	+14.6
1871	748	582.9	-1.9	+64	812	25.6
1906	965	581.5	+0.5	+17	982	4.9
1933	1,487	578.5	-2.5	-85	1,402	15.6
1945	1,294	580.1	+0.1	+3	1,297	-8.8

on 12.1 for a length from 1,200 feet to 3,600 feet south of the breakwater. The values shown in Table 4 can be added for a representative length of shoreline of 3,600 feet to yield the result that an accretion rate as high as 48,500 square feet per year in the period 1856 to 1871 decreased to a rate of about 6,000 square feet per year from 1871 to 1906, then increased again to 20,500 square feet per year following construction of the breakwater extensions after 1906, and finally showed an average erosion rate of 8,000 square feet per year from 1933 to 1945. This last value corresponds to an erosion rate of 0.75 foot per year as determined from analysis of the aerial photos. However, it should be emphasized that the recently observed erosion rates reflect two effects: (a) The length of shoreline near the harbor has been protected by rubble and groins, and (b) the unprotected shoreline farther south is backed by dunes with an average height of about 120 feet with peaks more than 200 feet above the lake level.

The rate of accretion at times on the south side may seem somewhat surprising, but it must be recalled that the littoral drift often reverses (see Fig. 22) and in some years may be completely reversed. The variable direction of littoral drift is also evidenced by the two surveys in Figure 12, which shows the harbor entrance shoal from the south side as being apparently larger than that from the north in 1973.

Using the approximation of 1 cubic yard of sediment per square foot of beach the 1950-73 observed average erosion rate for about 9,000 feet south of Holland Harbor is 0.75 cubic yard per year per foot of shoreline, plus the bluff contribution of  $0.75 \times 120/27 = 3.33$  cubic yards per year per foot for a total loss rate for unprotected shoreline of 4.08 cubic yards per year per foot of shoreline. When compared with the erosion rates observed for the shoreline about 1 mile or more north of Holland Harbor of 3.18 cubic yards per year per foot, the difference of 0.9 cubic yard per year per foot of 22 percent can be attributed to the navigation structure. The effect is very small and should not be expected to be readily apparent. The rate of loss of 0.9 cubic yard per year per foot of bluff material would correspond to a shoreline erosion rate of less than 0.2 foot per year for a bluff height of 120 feet.

The actual loss of land to the south of Holland (attributed to the navigation structure) is relatively small, at the most 22 percent. This figure has been derived as a 23-year average, but with current high lake levels the present natural erosion rate is certainly higher than the average.

The evolution of the shoreline at Holland was studied using the present model. The relevant physical data and the estimates of offshore sediment losses were used in the analysis. Interpolation of values shown in Table 1 gives the shoreline every 100 feet along the base line. The channel at the harbor entrance was collapsed to zero so that the south reach ended at 0- and the north at 0+. These shorelines indicate that the shore is stable at the breakwater; therefore, when the direction of transport is toward the breakwater it is assumed that the sand transported to the breakwater is entirely lost offshore. Monthly lake levels were taken from Figure 21. The results of these computations are not given since they are essentially previously described results. The average beach slope at the waterline was determined to be 1:10; the beach profiles in Figure 17 near the breakwater show that this is a reasonable estimate although the slopes are not constant from profile to profile. The height of the berm is assumed to be 10 feet. The depth to no sediment motion was estimated at 30 feet, based on visual consideration of the offshore bathymetry and the use of Weggel's method (J.R. Weggel, personal communication). An offshore loss of 3.2 cubic yards per year per foot of beach is also included (see Fig. 26).

The transport equation for this situation can be written (see eq. 53)

$$\frac{\partial y}{\partial t} = \frac{\partial}{\partial x} (K_D^2 Q) - \frac{1}{m} \frac{dD}{dt} - \frac{dL}{dt}$$

where

$$Q = \cos \alpha_o \sin \alpha_b \text{ and } \frac{\partial Q}{\partial x} = \frac{\partial}{\partial x} (K_D^2 Q)$$

m = beach slope at waterline

D = dimensionless lake level

$\frac{dL}{dt}$  = dimensionless offshore line loss

This equation will be applied on each side of the breakwater. When the incoming wave direction gives drift toward the breakwater, the boundary conditions expressed in Q are

$$\left. \frac{\partial Q}{\partial x} \right|_{x=0} = 0$$

and

$$Q \Big|_{x=\infty} = \cos \alpha \sin \alpha_b$$

Conversely, when the incoming wave direction gives drift away from the breakwater, the conditions become

$$Q \Big|_{x=0} = 0$$

and

$$Q \Big|_{x=\infty} = \cos \alpha \sin \alpha_b$$

Choice of wave climate is the remaining input parameter to be determined, and is the most controversial. The wave climate most desirable for the study of shoreline evolution is a time series giving wave height, H, period, T, and direction, D. Unfortunately, this is seldom available and hence monthly statistical summaries must be used, such as those by the SSMO for southern Lake Michigan. One possible use of the summaries is to construct monthly times t for each possible (H,T,D) triple, i.e., t(H,T,D), and then calculate the evolution of the shoreline as the (H,T,D) triples are chosen in some deterministic order or at random. This method would be computationally very expensive and is not used. The most simple approach is to assume that these are but two (H,D,T) triples representing the gross transport north and south, each occurring for some length of time per month. The entire shoreline is alternately calculated for an incremental time, assuming the direction of the incoming wave is positive, then negative. The period, T, used is taken to be the average T; i.e.,

$$\bar{T} = \frac{\sum p(H,T) T}{\sum p(H,T)}$$

where the p(H,T) are the (H,T) probabilities given in Table 19 of the SSMO (National Oceanic and Atmospheric Administration, 1963-73). The choice of (H,D) for north and south, denoted (H<sub>N</sub>,D<sub>N</sub>) and (H<sub>S</sub>,D<sub>S</sub>), respectively, must now be made. This choice is subject to the condition that the actual northerly transport, as calculated from the statistics and given a straight shoreline for the reach of interest, be preserved; i.e.,

$$t_N H_N^2 \bar{T} \cos \bar{\alpha}_O \sin \bar{\alpha}_b = t_n \sum_{\substack{H,T \\ \text{north transport}}} p(T|H) p(H,D) T H^2 \cos \alpha_O \sin \alpha_b$$

where

- $t_n$  = number of hours in a given month
- $p(T|H)$  = conditional probability T occurs given H
- $p(H,D)$  = probability of (H,D) pair (using Table 18 in SSMO as a data base)
- $\alpha_O$  = D<sub>N</sub> - shoreline orientation
- $\alpha_b$  = f( $\alpha_O$ )
- $t_N$  = number of hours the average wave condition exists
- $H_N$  = average wave height
- $\bar{\alpha}_O$  = D<sub>N</sub> - shoreline orientation
- $D_N$  = average direction

and similarly for the directions giving south transport.

The average directions of the shoreline at the breakwater are calculated from the historical records. The directions are chosen for the incoming wave angles since the complex geometry of the harbor breakwater shields the nearby shoreline from waves arriving from most directions. At present, the time duration of waves arriving from the north is assumed to be the same as from the

south; therefore,  $t_N = t_S = 0.5 t_z$ . The conservation of transport equation is then used to calculate the average wave heights  $H_N$  and  $H_S$ . The results of these calculations are given in Table 5.

Table 5. SSMO averages for Holland Harbor.<sup>1</sup>

Month	$H_S$ (ft)	$H_N$ (ft)	$\bar{T}$ (s)
Jan.	4.3	4.3	6.1
Feb.	4.0	3.6	6.0
Mar.	3.5	1.9	6.3
Apr.	2.6	2.4	5.5
May	2.3	2.1	5.4
June	2.1	1.8	5.3
July	1.8	2.1	5.3
Aug.	2.8	2.5	5.6
Sept.	3.0	2.6	5.8
Oct.	3.6	3.6	5.9
Nov.	4.0	3.4	6.0
Dec.	4.2	3.8	5.9
Annual	3.3	2.9	5.8

<sup>1</sup>For  $D_S = -33$ ;  $D_N = +27^\circ$ .

The computer program described in the Appendix was used to calculate the evolution of the shoreline from September 1967 to May 1968. The historical 1967 and 1968 shorelines, as well as the computed 1968 shoreline, are shown in Figure 29. The calculation assumes that  $\Delta x = 100$  feet with  $\lambda \approx 1$  which gives a value for  $\Delta t$  which varies from 8 to 20 hours depending on the monthly wave characteristics. The principal discrepancy between the predicted and actual 1968 shoreline occurs near the breakwater. Although the shapes agree, there is an erosion in the calculated shoreline which is probably due to the approximations used in the calculation of the diffraction coefficients, and incoming wave angles which are functions of  $x$  in the shadow region of the diffraction zone. The unaltered theory of Penny and Price (1944) was incorporated into the numerical scheme since most breakwaters can be represented as line barriers, and hence is almost always useful. However, for the case of Holland Harbor a universally valid prediction of the shoreline would require the detailed calculation of the diffraction effects due to the geometry of the breakwaters. Also, the convenient choice of incoming wave direction obscures the fundamental problem of how to properly use the statistical wave summaries.

#### IV. CONCLUSIONS AND RECOMMENDATIONS

The basic idea of Pelnard-Considere (1956), i.e., to investigate shoreline evolution by concentrating on conservation of mass as a special one-dimensional problem, has been generalized to essentially its limits of applicability. These physical processes of refraction and diffraction (where applicable) have been incorporated, including deterministic variations in lake level, bluff height, and beach slope. The inclusion of refraction makes possible the proper use of the known physical relationships between wave energy and littoral drift on a priori basis without necessarily determining these as results from the past recorded shorelines at a given location. Accurate determination of shore behavior in the lee of a breakwater requires inclusion of diffraction in some

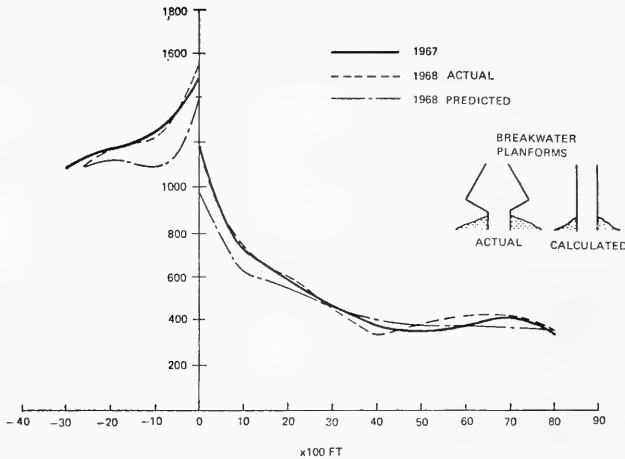


Figure 29. Computed data versus actual data.

form. This could be done in a heuristic manner, either in the global approximation described previously or in the use of the constant depth theory of Penny and Price (1952). It could also be done in a more rigorous manner which would include the effects of a sloping beach. Thus, quantitative predictions of the shoreline can, in theory, be attempted in situations where onshore-offshore transport of sand is either negligible or is known from other sources.

The resulting theory is presented in two equivalent forms; one in terms of the behavior of the shoreline  $y(x,t)$  alone, the other expressed explicitly in the longshore transport  $Q(x,t)$  and implicitly in  $y(x,t)$ . The former has the advantage that numerical schemes, such as that of Crank-Nicolson can qualitatively indicate the behavior of the shoreline in regions of rapid change. However, the conservation of mass is difficult, if not initially impossible to achieve since any approximation of a transport-derived term (i.e., a term arising from  $\partial Q/\partial x$ ) will alter the transport balance. The later form allows the use of analytical or numerical approximations in the transport equation which will not disturb the total sand content of the system, but only its local distribution.

The most severe and unavoidable limitations to the engineering application of these methods are the use of the statistical wave summaries. One possible use of these statistics was shown; however, many others are possible. Efficient and accurate use of the offshore wave statistics is endemic to the problem of large-scale shoreline prediction, and must be achieved before any theory (whether one line, multiple lines, or grid) can successfully produce accurate results.

The problem of shoreline evolution sensitivity to time step in the input wave climatology would require further research. Despite this limitation, if the effects of wave refraction, wave diffraction, and change of lake level are taken into account (as in this report), and if the method is generalized, then a mathematical model with multiple bottom contour lines could be formulated which would (if the problem of wave statistics input is solved) permit a calculation of the evolution of the complete bottom topography.

It is important to point out that wave refraction effect on shoreline evolution has been found particularly important. It is particularly necessary in order to determine a planform stability criteria which can be established from the present formulation.

The problem of shoreline stability needs to be investigated, both physically and numerically, as for some deepwater wave angle, shoreline perturbation may increase by instability instead of being flattened out.

Perhaps one of the most significant results of this mathematical approach to shoreline evolution is to point out the need for more research to quantify the phenomenology relevant to shoreline evolution. The insertion of empirical parameters has allowed the investigator to fit (to a large extent) a form of shoreline evolution; however, the processes involved in each of these parameters are not well known, and, what fits at Holland, may not necessarily apply elsewhere. For example, the research topics which will improve the model are (a) onshore-offshore movement; (b) quantity of sand (silt) lost by rip currents or density currents; (c) percentage of sand in suspension; (d) distribution of sand discharge as a function of the distance from shore; and (e) more importantly, how to treat the wave climatology in finite time intervals to obtain an equivalent result. The last topic may be the most difficult since the noise, (i.e., daily variation and effect of storm) may exceed the signal (i.e., the long-term trend). Shoreline evolution is due to a succession of extreme events separated by long-period time effects of equal importance. Therefore, the treatment of long-term evolution from an average wave climatology is questionable, since the complete time history may have to be considered on a daily basis. This topic can be investigated by a sensitivity analysis to wave definition; e.g., the present model could be used, as well as a research guideline for filling many knowledge gaps in shoreline processes.

## LITERATURE CITED

- COLE, A.L., and HILIKER, R.C., "Wave Statistics for Lake Michigan, Huron, and Superior," Department of Meteorology and Oceanology, University of Michigan, Ann Arbor, Mich., 1970.
- LE MEHAUTE, B., "A Theoretical Study of Waves Breaking at an Angle with a Shoreline," *Journal of Geophysical Research*, Vol. 66, No. 2, Feb. 1961, pp. 495-499.
- LE MEHAUTE, B., and KOH, R.C., "On the Breaking of Waves Arriving at an Angle to the Shore," *Journal of Hydraulic Research*, Vol. 5, No. 1, 1967, pp. 67-88.
- LE MEHAUTE B., and SOLDATE, M., "Mathematical Modeling of Shoreline Evolution," MR 77-10, U.S. Army, Corps of Engineers, Coastal Engineering Research Center, Fort Belvoir, Va., Oct. 1977.
- MOBAREK, I.E., and WIEGEL, R.L., "Diffraction of Wind Generated Waves," *Proceedings of the 10th Coastal Engineering Conference*, American Society of Civil Engineers, Ch. 13, Vol. I, 1966, pp. 185-206.
- NATIONAL OCEANIC AND ATMOSPHERIC ADMINISTRATION, "Summary of Synoptic Meteorological Observations (SSMO) for Great Lakes Areas," National Climatic Center, Asheville, North Carolina, 1963-73.
- PELNARD-CONSIDERE, R., "Essai de Theorie de l'Evolution des Formes de Rivage en Plages de Sable et de Galets," *Fourth Journees de l'Hydraulique, Les Energies de la Mer*, Question III, Rapport No. 1, 1956.
- PENNY, W.G., and PRICE, A.T., "The Diffraction Theory of Sea Waves and the Shelter Afforded by Breakwaters," *Philosophical Transactions*, Royal Society of London, Serial A, Vol. 244, 1952, pp. 236-253.
- SAVILLE, T., Jr., "Wave and Lake Level Statistics for Lake Michigan," TM-36, U.S. Army, Corps of Engineers, Beach Erosion Board, Washington, D.C., Mar. 1953.
- U.S. ARMY, CORPS OF ENGINEERS, COASTAL ENGINEERING RESEARCH CENTER, *Shore Protection Manual*, 3d ed., Vols. I, II, and III, Stock No. 008-022-00113-1, U.S. Government Printing Office, Washington, D.C., 1977, 1,262 pp.
- U.S. ARMY ENGINEER DISTRICT, DETROIT, "Detailed Project on Shore Damage for Holland Harbor, Michigan," Tetra Tech Report, Detroit, Mich., Apr. 1975.



# APPENDIX

## COMPUTER PROGRAM

This appendix presents the listing and brief explanation of the computer program written to investigate the behavior of a shoreline which contains a complete littoral barrier at  $x = 0$ . The numerical scheme is based on the finite-difference method of Crank-Nicolson, used to solve the cyclic nonlinear transport equations in  $Q$  and  $y$ . Although the program is written expressly for Holland Harbor, Michigan, hopefully, enough explanation is given to modify the program, if necessary, to suit a particular application.

The program consists of a main program, which is simply a calling routine to the controlling subroutine, and eight subroutines. The interrelationship of these programs is shown in the figure below; a brief discussion of each subroutine follows.

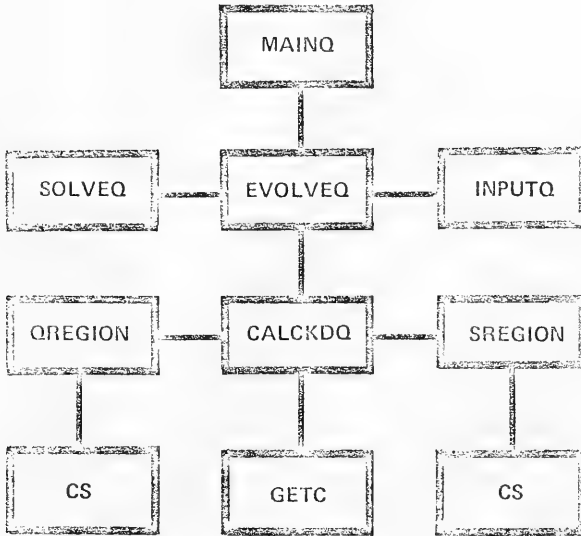


Figure. Program structure.

MAINQ    Calls subroutine EVOLVEQ

EVOLVEQ    The controlling subroutine which organizes the numerical method in a global sense and calls various other subroutines as required. The first call is to INPUTQ, which reads the controlling parameters, historical shorelines and lake levels, and statistical wave information. For each month in the time period of interest, subroutine CALCKDQ is called. (It is assumed that during a month the diffraction coefficients change negligibly.) For alternating equal incremental times the angle of the incoming waves is changed and subroutine SOLVEQ is called. This is repeated until a month's time has been completed. Then this is repeated until another historical shoreline is reached.

INPUTO This routine reads the information required to define a particular problem. Below are the cards required with an explanation of the variables required. Title cards are user information devices which are printed but never used. The card(s) are numbered by their order as defined by READ statements.

CARD 1: title card

CARD 2: LAMBDA =  $\lambda = \Delta\hat{t}/\Delta\hat{x}^2$

B = bluff height (feet)

DO = depth to no sediment motion (feet)

DX =  $\Delta x$  (feet)

BERM = berm height (feet)

BWL = length of breakwater (feet)

BWD = depth of breakwater tip (feet)

SLOPE = slope of shore profile at waterline

CARD 3: XLINE = offshore line loss (square feet per hour)

CARD 4: title card

CARD 5: N1 = number of grid points to left of breakwater

N2 = total number of grid points on both sides of the breakwater

ND = number of historical shorelines

NY = number of years lake levels are to read

INYR = year of the first historical shoreline (must be year of first lake level as well)

CARD 6: for all years with historical shorelines read

year (I); I = 1,ND

month (I); I = 1,ND

hour (I); I = 1,ND where hour is the day  $\times$  24

CARD 7: for each grid point I read historical shorelines (feet)

CARD 8: title card

CARD 9: for each year read lake level for each month

CARD 10: title card

CARD 11: for each month (including annual which is not at present used) input (in the notation used for Holland)  $H_S$ ,  $H_N$ ,  $D_S$ ,  $D_N$ ,  $\bar{T}$ ,  $\bar{T}$ .

The input data above are printed without explanation along with several assays used internally. Note that in this routine  $\lambda$  is redefined slightly so that a month's time is exactly  $2n\Delta t$ .

SOLVEQ This subroutine calculates the shoreline for one time step assuming a previous shoreline (and shoreline angle =  $\tan^{-1}(\partial y/\partial x)$ ) and diffraction coefficients as calculated in subroutine CALCKDQ. The scheme is essentially as is described in Section 2. The matrix inversion is achieved using a standard algorithm for tridiagonal matrices.

CALCKDQ This routine calculates the diffraction coefficient and incoming wave angle  $\alpha = \alpha(x)$  in the diffraction zone using the theory of Penny and Price (1952) for both incoming wave directions (the angle convention is shown in subroutine INPUTQ).

QREGION Calculates diffraction in the "Q" region.

SREGION Calculates diffraction in the "S" region.

CS Calculates complex valued Fresnel integral.

CETC Calculates a given depth and period.

Note I. In subroutine EVOLVEQ  
 L1 = 1st year index  
 L2 = last year index

Calculation

begins at date: year (L1), month (L1), hour (L1)  
 ends at date: year (L2+1), month (L2+1), hour (L2+1)

In a general program

L1 = 1  
 L2 = ND-1 where ND is defined in subroutine INPUTQ ND must be passed to subroutine EVOLVEQ.

Note II. Program as given in this report is set up to allow complete bypassing (lost offshore) when waves are not diffracted, i.e.,



To change program for no bypassing, four statements must be changed in subroutine SOLVEQ.

2 statements after 1001  
 change QOLD (N1P1) = (1-ID) × QOLD (N1P2)  
 to QOLD (N1P1) = 0

1 statement after 1001  
 change QOLD (N1) = (ID-1) × QOLD (N1M1)  
 to QOLD (N1) = 0

1 statement after 3000  
 change P(N1) = 1. - (1D-1) × Q(N1M1)  
 to P(N1) = 1

3 statements after 3000  
 change Q(N1P1) = 0 + (2-ID)/P(N1P1)  
 to Q(N1P1) = 0

```

PROGRAM MAINQ(INPUT,OUTPUT,TAPE3=INPUT,TAPE6=OUTPUT)
CALL EVOLVEQ
CALL EXIT
END
SUBROUTINE EVOLVEQ
COMMON/ HDATA/ LAMBDA,R+DQ,DX,HERM,N1,N2,BML,BWD,DXHAT,SLOPE,XLINE
COMMON/DIRP/ XN2(2+115),AA(2+115)
COMMON/ SSMU/ DIR(13+2),PER(13+2),OMH(13+2),XB(13+6),AMP(13+2)
COMMON /LAKELVL/ XL(24+12)
COMMON /SRLINE/ UATE(3+8),SL(115,A)
COMMON/ Z33/ Z3(13,2)
I=IENSUN X(115),Y(115),IC(115)+VX(115)+VY(115)+RSL(115)+MD(13)
REAL LAMBDA
DATA WD/31,28,31,30+31,30+31+30,31+30,31+30+31,365/
C
C L1=INDEX OF FIRST SHORELINE
L1=6
L2=6
C
C READ INPUT DATA
C
CALL INPUTQ
N1=N1+1
N1P=N1+1
N1P2=N1+2
N2=N1+2+1
IX=(N1-1)*DX+DX
DO 1001 I=1,N1
IX=IX+DX
1001 IC(I)=IX
IX=DX
N1P=N1+1
DO 1002 I=N1P,N2
IX=IX+DX
1002 IC(I)=IX
C
C DEFINE ORIGINAL SHOELINE AND SHORELINE ANGLE
C
F=1./(R+DQ)
DO 1100 I=1,N2
1100 Y(I)=SL(I,L1)*F
EQ=Q+5./(R+DQ)
Z=(Y(2)-Y(1))/DXHAT
VY(1)=ATAN(Z)
DO 1101 I=2,N1+1
Z=(Y(I+1)-Y(I-1))*EQ
1101 VY(I)=ATAN(Z)
Z=(Y(N1+1)-Y(N1M1))/DXHAT
VY(N1)=ATAN(Z)
Z=(Y(N1P2)-Y(N1P1))/DXHAT
VY(N1P1)=ATAN(Z)
DO 1102 I=N1P2,N2+1
Z=(Y(I+1)-Y(I-1))*EQ
1102 VY(I)=ATAN(Z)
Z=(Y(N2)-Y(N2M1))/DXHAT
VY(N2)=ATAN(Z)
C
C MAIN ANALYSIS LOOP
C
IYEAH=1
DO 9000 L=L1,L2
C
IY1=DATE(1,L)
IY1=DATE(2,L)
IY2=DATE(1,L+1)
IY2=DATE(2,L+1)
NMON=IY2-IY1*12+IM2-IM1+1
MUN=IM1-1
DO 2000 LL=1,NMON
MUN=MUN+1
IF(MUN .NE. 13) GOTO 1
MUN=1
IYEAH=IYEAH+1
1 IY1=XS(MON+5)
Z1=Z3(MON+1)
Z2=Z3(MON+2)
CALL CALCROU(Y+MUN)
DTHAT=XG(MON+3)
D1=NIM(MON+1)
D1P2=NIM(MON+2)
IF(LL .EQ. 1) GOTO 11
IF(LL .EQ. NMON) GOTO 12
DTHAT=XG(MON+4)
DTHAT=XG(MON+3)

```

7+1=L 0009 0D

```

      XL9=XS(MON,2)
      GOTO 10
11  X=M*(M+1)*24
      FACT=(X*DATE(3,1))/XM
      GOTO 13
12  X=M*(M+1)*24
      FACT=DATE(3,1)/XM
13  XL9=FACT*XS(MON,2)
      CT=FACT*XS(MON,4)
      DT=FACT*XS(MON,3)
14  DLLDT=AL(IYEAR+MON)/24.
      DLLH=DT*LLDOT/DT/(B*100)
      PRINT 149
140  FORMAT(1H1,/)
      PRINT 150+L1+YEAR,MON,ITLIM,DT*HAT,DLLHAT,DT
150  FORMAT(0 FOR PARAMETERS=316+* ITLIM,DT*HAT,DLLHAT,DT=*,I6,3E11,3)
      PRINT 151+MON,(/S(MON)*K),K(1+6)
151  FORMAT(/+* LISTING OF ANHY XS FOR MONTH*,I3+*P10,3)
      DXX=DLLHAT/SLOPE
      DD 2001 I=1,N2
      CALL SOLVE0(Y,VY,X,VX,Z1,XL9,DLLHAT,DT*HAT,1,AMP(MON,1),DT)
      CALL SOLVE0(X,VX,Y,VY,Z2,XL9,DLLHAT,DT*HAT,2,AMP(MON,2),DT)
2001  CONTINUE
C
C      PRINT SHOWELINE AT END OF MONTH
C
      JYEAR=IY1*(2+LL+2)+M1
      JMON=JYEAR/12*(JYEAR/12)+1
      JYEAR=JYEAR/12
      WRITE(6,200) JYEAR,JMON
200  FORMAT(/+* FOR YEAR*,I3+* MONTH*,I3+* LISTING OF FINAL SHORELINE
1*)
      DD 3000 I=1,N2
3000  RSL(I)=Y(I)/F
      DD 3001 I=1,6
      J1=(I-1)*15+1
      J2=J1+14
      IF(I .EQ. 8) J2=115
      WRITE(6,201) (I(J)+J0J1,J2)

201  FORMAT(///+* X      +*1518)
      WRITE(6,202) (RSL(J)+J0J1,J2)
202  FORMAT(/+* Y      +*15F8.1)
3001  CONTINUE
2000  CONTINUE
9000  CONTINUE
      RETURN
      END
SUBROUTINE SOLVE0(Y,Y,X,X,SLANG,Z3,XL9,DLLHAT,DT*HAT,IO,AMP,DT)
C
C      SOLVE FOR ARRAY XX USING IMPLICIT SCHEME FOR TRANSPORT QNEW
C
      COMMON/BDATA/ LAMBDA,H,DO,DX,PERM,N1,N2,BWL,BWD,DXHAT,SLOPE,XLINE
      COMMON/CFPC/  XND2(2+115),AA(2+115)
      DIMENSION XX(115),YY(115),V(115),SLANG(115),YULU(115),VV(115)
      DIMENSION P(115),W(115),L(115),V(115),D(115),QNEW(115),QOLD(115)
      REAL
      E=2.0*DXHAT
      E=1./EB
      N1M=1
      N1P=1+1
      N1P2=N1+2
      N2M=1+2=1
      DJ 1000 I=1,N2
1000  YLD(I)=YY(I)
C
C      CALCULATE OLD U (WOLD) BASED ON OLD SHORELINE AND PRESENT DIRECTION
C
      DD 1001 I=1,N2
      V(I)=V(I)
      A1G=AA(ID+I)+V(I)
      BANG=ANGL*Z3
1001  QOLD(I)=AMP*COS(ANG)*SIN(BANG)*XND2(ID,1)
      QOLD(N1)=(ID-1)*QOLD(N1M1)
      QOLD(N1P1)=(2-ID)*QOLD(N1P2)
      A1G=AA(ID,1)
      BANG=ANG*Z3
      QI=1+AMP*COS(ANG)*SIN(BANG)*XND2(ID,1)

```

```

A=GA(1D+N2)
B=NG*NG*Z3
Q(LM)=P*AM* $\cos(\text{ANG})$ *SIN(BANG)*XXD2(1D+N2)
ITLAST=3
D) 9999 IT=1,ITLAST
C
C CALCULATE ARRAYS L+D
C
D) 2000 I=2,N1M1
X=X* $\Delta t^2$ (10,1)
E=(Y(I+1)-Y(I=1))*E9
A=GA(1D+I)+VV(I)
B=NG* $\Delta t$ *Z3
C=A*E*(Z3* $\cos(\text{ANG})$ * $\cos(\text{BANG})$ =SIN(ANG)*SIN(BANG))/(1,+E*E)
2000 L(1)=XL9+C*XX
D) 2001 I=N1P2+N2M1
X=X* $\Delta t^2$ (10,1)
E=(Y(I+1)-Y(I=1))*E9
A=GA(1D+I)+VV(I)
B=NG* $\Delta t$ *Z3
C=A*E*(Z3* $\cos(\text{ANG})$ * $\cos(\text{BANG})$ =SIN(ANG)*SIN(BANG))/(1,+E*E)
2001 L(1)=XL9+C*XX
D) 2002 I=2,N1M1
D(1)=QOLD(I)+L(I)*(WOLD(I+1)=2,+QOLD(I)+QOLD(I+1)2)
D) 2003 I=N1P2+N2M1
D(1)=QOLD(I)+L(I)*(WOLD(I+1)=2,+QOLD(I)+WOLD(I+1)2)
D(1)=QOLD(I)
D(N1)=C(N1P1)=0.
D(N2)=GLIM*2
C
C CALCULATE ARRAYS P+Q
C
P(1)=1.
Q(1)=0.
D) 3000 I=2,N1M1
P(1)=L(1)*(-Q(I=1)+2.)+1.
Q(1)=L(1)/P(1)
P(N1)=1.+(1D=1)*Q(N1M1)
P(N1P1)=1.
Q(N1P1)=0.+(2-ID)/P(N1P1)
D) 3001 I=N1P2+N2M1
P(1)=L(1)*(-Q(I=1)+2.)+1.
Q(1)=L(1)/P(1)
P(N2)=1.
C
C SOLVE FOR TRANSPORT QNEW
C
U(1)=R(1)/P(1)
D) 4000 I=2,N1M1
U(1)=R(1)+L(1)*R(1)/P(1)
QNEW(N1)=U(N1)=D(N1)/P(N1)
D) 4001 I=1,N1M1
J=N1-1
QNEW(J)=R(J)+QNEW(J+1)+U(J)
U(N1P1)=D(N1P1)/P(N1P1)
D) 4002 I=N1P2+N2M1
U(1)=R(1)+L(1)*R(1)/P(1)
QNEW(N2)=U(N2)=D(N2)/P(N2)
D) 4003 I=N1P1+N2M1
J=N2-1
QNEW(J)=R(J)+QNEW(J+1)+U(J)
IP=N1+Q
IF(IP=INT ,EQ. 0) GOTO 50
PRINT 400
400 FU=MAT(/,* LISTING OF QNEW*)
PRINT 401+(QNEW(1)+I=1,N2)
401 FU=MAT(1X+1D10,0)
C
C CALCULATE NEW SHORLINE
C
50 XX(1)=0.5*(QNEW(2)+QNEW(1)+QOLD(2)+QOLD(1))
D) 5000 I=2,N1M1
XX(1)=0.25*(QNEW(I+1)+QNEW(I=1)+QOLD(I+1)+QOLD(I=1))
XX(N1)=0.5*(QNEW(N1)+QNEW(N1=1)+QOLD(N1)+QOLD(N1=1))
XX(N1P1)=0.5*(QNEW(N1+2)+QNEW(N1+1)+QOLD(N1+2)+QOLD(N1+1))
D) 5001 I=N1P2+N2M1
XX(1)=0.25*(QNEW(I+1)+QNEW(I=1)+QOLD(I+1)+QOLD(I=1))
XX(N2)=0.5*(QNEW(N2)+QNEW(N2=1)+QOLD(N2)+QOLD(N2=1))
FU=1/MAT/DX*AT
F1=D(LMAT/8LOPE
F2=XLTIME*UT/(H*Dn)**2
D) 5002 I=1,N2
XX(1)=F*XX(1)+Y(I)=F1+F2
Z=(XX(2)=XX(1))/DX*AT

```

```

SLANG(1)=ATAN(Z)
DO 5003 I=2,N1*1
Z=(XX(I+1)-XX(I-1))*E9
5003 SLANG(I)=ATAN(Z)
Z=(XX(N1)-XX(N1-1))/DXHAT
SLANG(N1)=ATAN(Z)
Z=(XX(N1+2)-XX(N1+1))/DXHAT
SLANG(N1+1)=ATAN(Z)
DO 5004 I=N1*2,N2*1
Z=(XX(I+1)-XX(I-1))*E9
5004 SLANG(I)=ATAN(Z)
Z=(XX(N2)-XX(N2-1))/DXHAT
SLANG(N2)=ATAN(Z)
IF (IT .EQ. ITLAST) GOTO 9999
DO 6000 I=1,N2
VV(I)=SLANG(I)
6000 VOLD(I)=XX(I)
9999 CONTINUE
RETURN
END
SUMMATION TIME CALC MOD(Y,MUN)
COMMON/ BDATA/ LAMBDA,R,DO,DX,HERM,N1,N2,BWL,BWD,DXHAT,SLOPE,XLINE
COMMON/ OIPRC/ XND(2+1),AA(2+1)
COMMON/ SSU/ DIR(1+2),PER(1+2),DMH(1+2),XS(1+2),AMP(1+2)
DIMENSION YY(115)
REAL *3
DAP=0.5/DXHAT
N1*1=N1+1
C
C
C
CALC DIFFRACTION FOR LH#
A=DIR(MON+1)
CALL GETC(RWD,PER(MUN+1),*3)
XX=X
DO 1000 J=1,N1
I=1+J
J=I+1
XX=X+DX
Y=R*L*YY(I)*E(B+D0)
R1=X*Y+Y*Y
R1=SQRT(R1)/*3
Z=X/Y
A1=ATAN(Z)
IF (A1 .LT. A) GOTO 1
CALL nREGION(M1,A,A1,*3)
AA(1+J)=A
GOTO 2
1 CALL sREGION(M1,A,A1,*3)
AA(1+J)=A1
2 XKD2(1+J)=K3*K3
1000 CONTINUE
DO 1001 I=N1*1,N2
XKD2(1+I)=1.
1001 AA(1+I)=A
C
C
C
CALC DIFFRACTION FOR HB#
A=DIR(MUN+2)
CALL GETC(RWD,PER(MUN+2),*3)
XX=X
DO 2000 I=N1*1,N2
I=I+DX
Y=R*L*YY(I)*E(B+D0)
R1=X*Y+Y*Y
R1=SQRT(R1)/*3
Z=X/Y
A1=ATAN(Z)
IF (A1 .LT. A) GOTO 11
CALL nREGION(M1,A,A1,*3)
AA(2+I)=A
GOTO 12
11 CALL sREGION(M1,A,A1,*3)
AA(2+I)=A1
12 XKD2(2+I)=K3*K3
2000 CONTINUE
DO 2001 I=1,N1
XKD2(2+I)=1.
2001 AA(2+I)=A
RETURN
END
SUMMATION TIME INPUTS
COMMON/ BDATA/ LAMBDA,R,DO,DX,HERM,N1,N2,BWL,BWD,DXHAT,SLOPE,XLINE
COMMON/ SMLINE/ UATE(3+8)+SL(115,A)

```

```

CMMUN/ LAKELVL/ XL(24,12)
CMMUN/ SMO/ DIR(13,2)+PER(13,2),DWH(13,2)+XS(13,6)+AMP(13,2)
CMMUN/ ZSS/ZS(13,2)
DIMENSION ZL(24,12)+MD(13)+ALIST(10)
REAL LAMBDA+LAMBDA*
DATA ND/31,28,31,30,31,30,31,31,30,31,30,31,31,30,31,30,31,365/

C PRINT 999
999 FERMAT(1M1,0 DATA AS HEAD BY SUBROUTINE INPUT0,/)

C
C READ SPACIAL PARAMETERS
C
C READ(5,101) (ALIST(I),I=1,10)
101 FERMAT(10AR)
READ(5,100) LAMBDA+B+DO+DX+BERM+RWL+RWD+SLOPE
130 FERMAT(8F10,1)
READ(5,100) XLINE
PRINT 101,(ALIST(I),I=1,10)
PRINT 100,LAMBDA,B+DO+DX+BERM+RWL+RWD+SLOPE+XLINE
C READ HISTORICAL SHORTLINE DATA
C
C READ(5,101) (ALIST(I),I=1,10)
READ(5,102) N1+N2+ND+NY,INR
102 FERMAT(6I10)
READ(5,100) ((DATE(J,I),I=1,ND),J=1,3)
DO 1000 I=1,N2
READ (5,100) (SL(I,J),J=1,ND)
1000 CONTINUE
PRINT 101,(ALIST(I),I=1,10)
PRINT 100,((DATE(J,I),I=1,ND),J=1,3)
DO 2000 I=1,N2
2000 PRINT 100,(SL(I,J),J=1,ND)

C
C READ HISTORICAL LAKE LEVELS AND COMPUTE DLL/DT
C
C F=1,(B+DO)
READ(5,101) (ALIST(I),I=1,10)
DO 1001 I=1,NY
READ(5,100) (ZL(I,J),J=1,12)
1001 CONTINUE

PRINT 101,(ALIST(I),I=1,10)
DO 2001 I=1,NY
IF=I+NYR=1
2001 PRINT 998,1P ,(ZL(I,J),J=1,12)
998 FERMAT(17,5X,12F10,2)
K=0
DO 1002 I=1,NY
IV=I+YR=I+1
LV=IV+4=(IV/4)
K=K+1
XL(I,1)=(ZL(I,2)-ZL(I,1))/MD(1)
M=1/(1+LV)
SF=MD/2+M
XL(I,2)=(ZL(I,3)-ZL(I,2))/XM
DO 1002 J=1,11
XL(I,J)=(ZL(I,J+1)-ZL(I,J))/MD(J)
IF(I,EU,NY) GOTU 1002
XL(I,12)=(ZL(I+1,1)-ZL(I,12))/MD(12)
1002 CONTINUE

C READ DIRECTIONS, P-MOODS, WAVE HEIGHTS FOR EACH MONTH
C
C
C DIRECTION CONVENTIONS
C
C
C 2 DEEP WATER ANGLE LESS THAN 0
C X DEEP WATER ANGLE GREATER THAN 0
C
C
C
C
C
C
C
C XXXXXXXXXXXXXXX

C Q=3,415926,1R0,
READ(5,101) (ALIST(I),I=1,10)
DO 1003 M=1,13
READ(5,100) DWH(M,1)+DWH(M,2)+DIR(M,1)+DIR(M,2)+PER(M,1)+PER(M,2)
DIR(M,1)=DIR(M,1)*CQ

```



```

1003 DIR(M,2)=DIR(M,2)*C9
PRINT 101:(ALIST(I)+I*10)
D0 2003 M*1+13
DIR1=DIR(M,1)/C0
DIR2=DIR(M,2)/C0
2003 PRINT 100:D*H(M,1)+D*H(M,2)+DIR1*DIR2*PER(M,1)+PER(M,2)
C
C CALCULATE PARAMETERS FOR SCALING
C
PRINT 200
F)HAT/,* LISTING OF SCALE PARAMETERS AS CALCULATED IN SUBROUTINE
1 INPUT*
D0 1004 M*1+13
Z1=0.25+5.5*0*H(M,1)/(5.1248*PER(M,1)**2)
Z2=0.25+5.5*0*H(M,2)/(5.1248*PER(M,2)**2)
A1=476.83*0*H(M,1)**2*PER(M,1)
A2=476.83*0*H(M,2)**2*PER(M,2)
A=A1
IF(A2 .GT. A1) A=A2
X3(M,1)=DXHAT*(B+D0)
DIRHAT=LAMBDA*DXHAT**2
DIRHAT1=(R+D0)**3/A
Y)=H(M)*12
N=XY/DY*1
1=N
C
C
DT=XY/N
X3(M,2)=LAMBDA*H(DY/DX**2)*A/(B+D0)
X3(M,3)=DIRHAT=LAMBDA*DXHAT**2
X3(M,4)=DT
X3(M,5)=N
X3(M,6)=H(M,0)*(R+D0)/A
X3(M,7)=1248*PER(M,1)*PER(M,1)
Z1(M,1)=0.25+5.5*0*H(M,1)/X10
Z1(M,2)=0.25+5.5*0*H(M,2)/X10
A*(M,1)=A1/A
A*(M,2)=A2/A
PRINT 201:M*(X3(M,K)+K*1.6)+Z1(M,1)+Z1(M,2)+AMP(M,1)+AMP(M,2)
201 PRINT*(MONTM=,13)* ARRAY XSA*3F0.3,F0.1,F5.0,F6.3,* ARRAY Z3**
1.2F0.3,* ARRAY AMP**2F6.3)
1004 CONTINUE
RETURN
END
SUBROUTINE QREGION(H,A,A1,K3)
C
C CALCULATES KD IN S REGION
C (ASSUMES H = DISTANCE/WAVE LENGTH)
C
REAL *3
PI=3.1415926535
C3=2.42427125
ST=SIGN((A1-A)/2.0)
S1=SIGN((A1+A)/2.0)
C2=COS(A1+A)
C1=COS(A1-A)
R3=S*PI*W)
U1=C3*H3*S7
U2=C3*H3*S8
X=PI*W*U1/2.
CALL CS(X,S6,C6)
V1=(1.-S6+C6)/2.0
W1=(S6+C6)/2.
X=PI*W*U2/2.
CALL CS(X,S6,C6)
V2=(1.-S6+C6)/2.0
W2=(S6+C6)/2.
X4=2.*PI*H*C1
X5=2.*PI*H*C2
C4=COS(X4)
C5=COS(X5)
S4=SIGN(X4)
S5=SIGN(X5)
D4=V1+C4*V2*C5*W1+S4*W2*S5
D5=V1+C4*W2*C5*V1+S4*W2*S5
K1=D4*U4+U5*U5
K1=SQR(K1)
RETURN
END
SUBROUTINE QREGION(H,A,A1,K3)
C
C CALCULATES KD IN Q REGION
C (ASSUMES H = DISTANCE/WAVE LENGTH)
C
REAL *3

```

```

PI=3.1415926535
C3=2*PI*27125
S7=BI*((A1+A)/2.)
S8=SI*((A1+A)/2.)
I1=COS(A1-A)
I2=COS(A1+A)
F3=SI*PI
U1=C1*43*S7
U2=C1*43*S8
X=PI*11*U1/2.
CALL CS(X+S6*C6)
I1=(1.-S6*C6)/2.
W1=(S6*C6)/2.
X=PI*11*U2/2.
CALL CS(X+S6*C6)
V2=(1.-S6*C6)/2.
A2=(S6-C6)/2.
X4=2*PI*W1*C1
X5=2*PI*W1*C2
C4=COS(X4)
C5=COS(X5)
S4=SI(X4)
S5=SI(X5)
C4C4=V1*C4=1*S4+V2*C5+W2*S5
C5=2*V1*S4=1*C4+V2*S5+W2*C5
W3=D4*U4+U4*O5
K3=SI*PI(K3)
RETURN
END
SJMROUTINE GETC(D,T,M3)

GIVEN DEPTH(D); PERIOD(T) CALCULATE WAVE LENGTH(M3)

G3=32./2
PI=3.1415926535
PI2=PI*PI
W3=G3*T/PI2
Z3=PI2*D*U1
X5=4*PI2*D*U/(G3*T)
Y3=I4*U(X3)
IF(X3.LT.10.0) GOTO 1
C3=G3*T/PI2
GOTO 2
1 Y3=EXP(X3)
T3=(Y3+1)/(Y3+1)
C3=G3*T*BI*U1(T3)/PI2
D3=10*U1=1+50
X5=2*Z3/C3
Y3=EXP(X5)
T3=(Y3+1)/(Y3+1)
D3=3*T3
X1=4*S(C3*D3)
X2=0.001*4*S(D3)
IF(X1.LT.X2) GOTO 2
C3=(C3+D3)/2.
CONTINUE
M3=C3*T
WRITE(S,100) M3,C3,D,T
100 FJ=HAT(/=0 ERROR IN COMPUTATION OF WAVE LENGTH=4*PI*0.3* CALL EXIT
)
2 CALL EXIT
M3=C3*T
RETURN
END
SJMROUTINE CS(X,S6,C6)
Z3=4*S(X)
IF(Z3.GT.4.0) GOTO 1
C6=SI*U1(Z3)
S6=Z3*C6
Z4=(4.-Z3)/(4.+Z3)
C1=((5.100778E=11*Z3+S.244247E=9)*Z3+5.451142E=7)*Z3+3.273308E=5)
C2=C0*(((C3*Z3+1.020418E=3)*Z3+1.107504E=2)*Z3+1.840965E=1)
S1=((6.077481E=10+Z3*5.883158E=8)*Z3+S.051141E=6)*Z3
S6=S6*(((S1*2.441810E=4)*Z3+6.12132E=3)*Z3+8.02649E=2)
GOTO 2
1 C3=COS(Z3)
S3=SI(Z3)
Z3=4./Z3
A3=((1.78258E=0*Z3+4.169289E=3)*Z3+7.970046E=3)*Z3+6.792801E=3)
A3=((4.3*Z3-3.09334E=4)*Z3+5.972151E=3)*Z3+1.6006428E=5)*Z3=
12.493422E=2
A1=3*Z3+4.440091E=9
A3=((1.7*6.33928E=4*Z3+5.401409E=3)*Z3+7.27169E=3)*Z3+7.428246E=3)
A3=((1.83*Z3+4.027145E=4)*Z3+9.31401E=3)*Z3+1.207998E=6)*Z3
H3=H1+1.994711E=1
Z3=SI*U1(Z3)
C3=0.45*Z3*(C3+A3+83*H3)
S3=0.45*Z3*(S3+A3+C3*H3)
2 RETURN
END

```

Le Mehaute, Bernard

A numerical model for predicting shoreline changes / by Bernard Le Mehaute and Mills Soldate. -- Fort Belvoir, Va. : U.S. Coastal Engineering Research Center ; Springfield, Va. : available from National Technical Information Service, 1980.

[72] p. : ill. : 27 cm. -- (Miscellaneous report -- U.S. Coastal Engineering Research Center ; no. 80-6) (Contract -- U.S. Coastal Engineering Research Center ; DACW72-77-C-0002); also Tetra Tech, Inc., report no. TC-831.

Includes bibliographical references.

A mathematical model for long-term, three-dimensional shoreline evolution is developed; a computer program is applied to a test case at Holland Harbor, Michigan.

1. Currents.
  2. Great Lakes.
  3. Holland Harbor, Michigan.
  4. Shoreline changes.
  5. Wave diffraction.
  6. Wave refraction.
- I. Title. II. Soldate, Mills. III. Series: U.S. Coastal Engineering Research Center. Miscellaneous report no. 80-6. IV. Series: U.S. Coastal Engineering Research Center. Contract DACW72-77-C-0002. V. Series: Tetra Tech, Inc., report no. TC-831.

no. 80-6

627

TC203

.U58lmr

Le Mehaute, Bernard

A numerical model for predicting shoreline changes / by Bernard Le Mehaute and Mills Soldate. -- Fort Belvoir, Va. : U.S. Coastal Engineering Research Center ; Springfield, Va. : available from National Technical Information Service, 1980.

[72] p. : ill. : 27 cm. -- (Miscellaneous report -- U.S. Coastal Engineering Research Center ; no. 80-6) (Contract -- U.S. Coastal Engineering Research Center ; DACW72-77-C-0002); also Tetra Tech, Inc., report no. TC-831.

Includes bibliographical references.

A mathematical model for long-term, three-dimensional shoreline evolution is developed; a computer program is applied to a test case at Holland Harbor, Michigan.

1. Currents.
  2. Great Lakes.
  3. Holland Harbor, Michigan.
  4. Shoreline changes.
  5. Wave diffraction.
  6. Wave refraction.
- I. Title. II. Soldate, Mills. III. Series: U.S. Coastal Engineering Research Center. Miscellaneous report no. 80-6. IV. Series: U.S. Coastal Engineering Research Center. Contract DACW72-77-C-0002. V. Series: Tetra Tech, Inc., report no. TC-831.

no. 80-6

627

TC203

.U58lmr

Le Mehaute, Bernard

A numerical model for predicting shoreline changes / by Bernard Le Mehaute and Mills Soldate. -- Fort Belvoir, Va. : U.S. Coastal Engineering Research Center ; Springfield, Va. : available from National Technical Information Service, 1980.

[72] p. : ill. : 27 cm. -- (Miscellaneous report -- U.S. Coastal Engineering Research Center ; no. 80-6) (Contract -- U.S. Coastal Engineering Research Center ; DACW72-77-C-0002); also Tetra Tech, Inc., report no. TC-831.

Includes bibliographical references.

A mathematical model for long-term, three-dimensional shoreline evolution is developed; a computer program is applied to a test case at Holland Harbor, Michigan.

1. Currents.
  2. Great Lakes.
  3. Holland Harbor, Michigan.
  4. Shoreline changes.
  5. Wave diffraction.
  6. Wave refraction.
- I. Title. II. Soldate, Mills. III. Series: U.S. Coastal Engineering Research Center. Miscellaneous report no. 80-6. IV. Series: U.S. Coastal Engineering Research Center. Contract DACW72-77-C-0002. V. Series: Tetra Tech, Inc., report no. TC-831.

no. 80-6

627

TC203

.U58lmr

Le Mehaute, Bernard

A numerical model for predicting shoreline changes / by Bernard Le Mehaute and Mills Soldate. -- Fort Belvoir, Va. : U.S. Coastal Engineering Research Center ; Springfield, Va. : available from National Technical Information Service, 1980.

[72] p. : ill. : 27 cm. -- (Miscellaneous report -- U.S. Coastal Engineering Research Center ; no. 80-6) (Contract -- U.S. Coastal Engineering Research Center ; DACW72-77-C-0002); also Tetra Tech, Inc., report no. TC-831.

Includes bibliographical references.

A mathematical model for long-term, three-dimensional shoreline evolution is developed; a computer program is applied to a test case at Holland Harbor, Michigan.

1. Currents.
  2. Great Lakes.
  3. Holland Harbor, Michigan.
  4. Shoreline changes.
  5. Wave diffraction.
  6. Wave refraction.
- I. Title. II. Soldate, Mills. III. Series: U.S. Coastal Engineering Research Center. Miscellaneous report no. 80-6. IV. Series: U.S. Coastal Engineering Research Center. Contract DACW72-77-C-0002. V. Series: Tetra Tech, Inc., report no. TC-831.

no. 80-6

627

TC203

.U58lmr



NOV 12 1980

